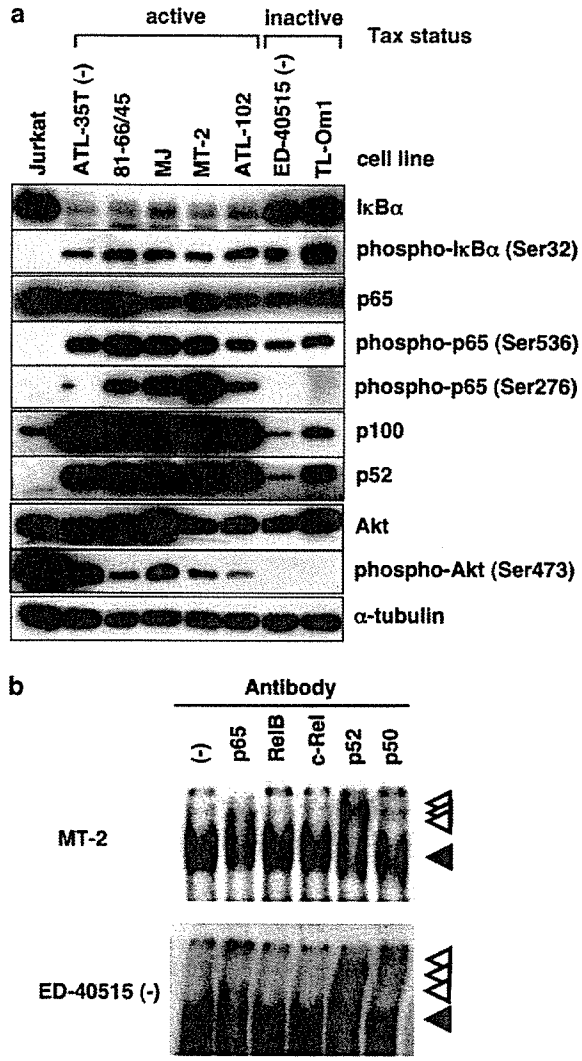

Figure 1 Constitutive NF-κB activation in HTLV-1-infected T-cell lines and ATL-derived cell lines. (**a**) Constitutive phosphorylation of IκBα, p65 and Akt. The whole cell-extracts obtained from the HTLV-1-infected T-cell lines (ATL-35T(−), 81–66/45, MJ, MT-2) and 3 ATL-derived cell lines (ATL-102, ED-40515(−), TL-Om1). Immunoblotting analyses were performed with antibodies against IκBα, phospho-IκBα, p65, phospho-p65, phospho-p65, p100/p52, Akt, phospho-Akt and α-tubulin (internal control). (**b**) Constitutive activation of NF-κB. The nuclear extracts were prepared from MT-2 and ED-40515(−) cell lines and EMSA was performed with specific DNA probe containing the NF-κB sequence. The results of supershift analysis using antibodies against each NF-κB subunits are shown. Closed and open arrowheads indicate positions of the specific DNA-NF-κB complex and the supershifted complex, respectively.

Tax-active cell lines, but not in Tax-inactive and control cell lines. The phosphorylation of p65 at Ser 276, which is not mediated by IKK,[26] was not correlated with IκBα phosphorylation. Constitutive phosphorylation of Akt at Ser473 was observed in five Tax-active cell lines and Jurkat.

We then performed EMSA using specific probes containing NF-κB binding sequence in the HIV-1 LTR promoter. The results revealed that NF-κB was constitutively activated in these HTLV-1-infected T-cell lines and ATL-derived cell lines, but not in Jurkat cells (Figures 1b and 2d). Representative results of MT-2 (Tax-active) and ED-40515 (−) (Tax-inactive) cells are shown in Figure 1b. Figure 1b also shows the result of supershift analysis using competitive antibody against each NF-κB subunit. In both cells, constitutive DNA binding of NF-κB was detected without any stimuli, and supershift bands were observed by addition of antibodies against p65, p52 or p50, indicating that activated NF-κB consisted of p65, p52 and p50 but not RelB or c-Rel.

Inhibitory effects of ACHP on NF-κB activation

We then examined the inhibitory effect of ACHP, a specific inhibitor for IKKβ and IKKα, on the phosphorylation of IκBα and p65 in these cell lines. Representative results are shown in Figure 2a with MT-2 and ED-40515(−) cells. ACHP efficiently inhibited phosphorylation of IκBα and p65 (IC_{50} values in MT-2 cells were 0.4 and 0.2 μM, respectively. IC_{50} values in ED-40515 (−) cells were 10.2 and 29.5 μM, respectively. See the Supplementary Information). Inhibitory effect of ACHP was observed as early as 5 min after the treatment (Figure 2b). It is noted that ACHP-treated MT-2 cells appeared to have an increasing net amount of IκBα concomitantly with the inhibition of IκBα phosphorylation. ACHP also exhibited similar effects with other Tax-active cell lines (data not shown). On the other hand, in ED-40515(−) cells, the amount of IκBα remained at the same level and the inhibitory dose was higher than MT-2 cells. In Figure 2c, the inhibitory effect of ACHP on other kinases involved in NF-κB pathways and other major signal transduction pathways are shown. ACHP showed no effect on phosphorylation of IKKα at Ser 181, processing of p100/p52, or phosphorylation of p65 at Ser 276. Moreover, ACHP did not inhibit the phosphorylation of p38 MAPK, ATF-2 and JNK. Unexpectedly, ACHP inhibited the phosphorylation of Akt (IC_{50} values were 4.5 μM. See the Supplementary Information), which is presumably responsible for the cytotoxic effect of ACHP on Jurkat cell survival. In Figure 2d, the inhibitory effect of ACHP on the DNA-binding activity of NF-κB was examined in MT-2, ED-40515(−) and Jurkat cells, using specific probes containing NF-κB binding sequence in the HIV-1 LTR promoter. In MT-2 cells, the NF-κB DNA binding was decreased by ACHP at greater than 1 μM. On the other hand, in ED-40515(−) cells, where the NF-κB DNA binding was weaker than MT-2, the significant inhibitory effect of ACHP was not observed until 50 μM.

Inhibitory effect of ACHP on expression of NF-κB target genes

In ATL, constitutive transcription of antiapoptotic genes such as *bcl-x_L*, *XIAP*, *c-IAPs* and *survivin* has been reported and ascribed to the resistance against anticancer agents.[27,28] NF-κB is known to be involved in the proliferation of HTLV-1-infected cell lines and fresh ATL cells by upregulating growth-promoting genes such as *cyclin D1*.[29] In addition, NF-κB stimulates the expression of *ICAM-1* and *VCAM-1* genes, which mediate T-cell activation and proliferation.[9,30]

As shown in Figure 3a, a distinct inhibition of *cyclin D1* gene expression was observed in MT-2 and ED-40515 (−) cells. Inhibition of *bcl-x_L*, *bcl-2*, *XIAP*, *c-IAP1* and *survivin* gene expressions was observed at high concentration of ACHP. These findings were also reproducibly observed using quantitative real-time RT-PCR analysis (data not shown), although we do not currently know the reason of the different susceptibilities of individual genes to ACHP. In Jurkat cells, inhibition of these gene expressions was weaker than ATL cell lines even at high concentration of ACHP. Figure 3b and c demonstrate that ICAM-1 and VCAM-1are highly expressed in MT-2 and ATL-102 cells, and that significant inhibitory effect was evident even at 1 μM ACHP. Whereas ACHP downregulated the expression of VCAM-1

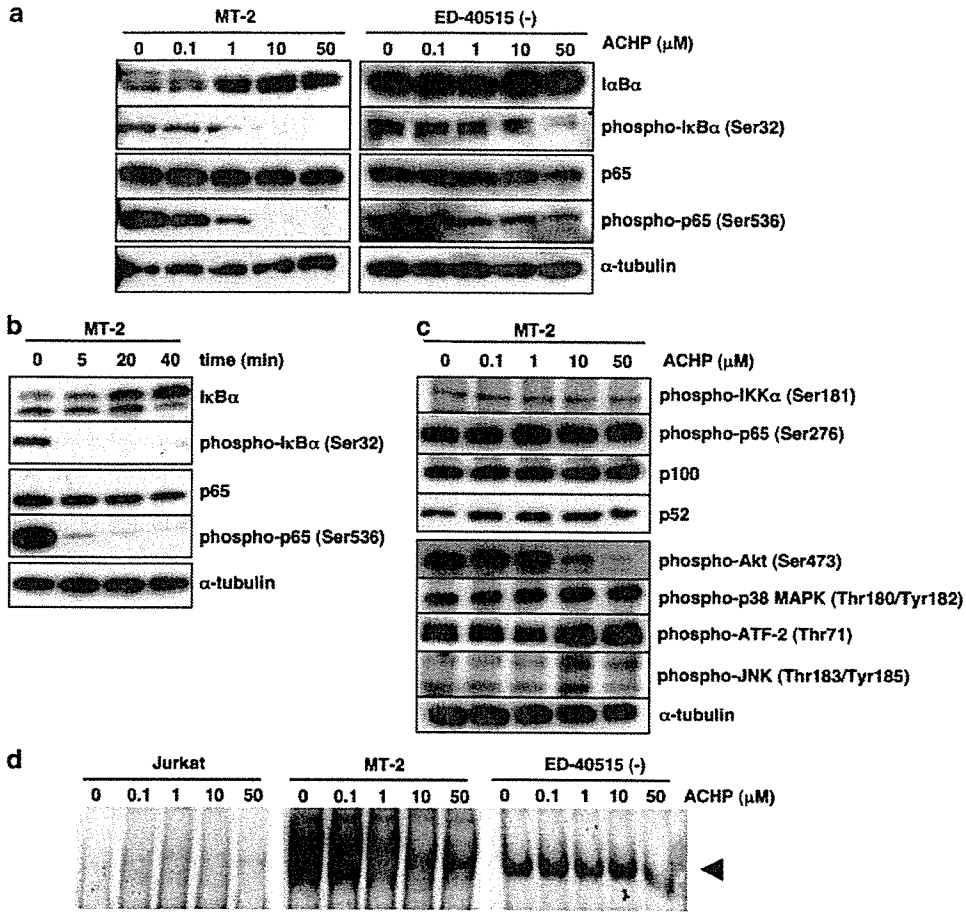

Figure 2 Inhibitory effects of ACHP. (**a**) Dose-dependent inhibition of IκBα and p65 phosphorylation. MT-2 and ED-40515(−) cells were treated with ACHP (0–50 μM) for 20 min and were subjected to immunoblotting analyses with the indicated antibodies. (**b**) Time-course of inhibition of IκBα and p65 phosphorylation. MT-2 cells were treated with ACHP (10 μM) and whole-cell extracts were subjected to immunoblot analysis. (**c**) Specificity of ACHP on IKK and other kinases. MT-2 cells were treated with ACHP (0–50 μM) for 20 min and were subjected to immunoblot analysis with the indicated antibodies. (**d**) Inhibition of NF-κB DNA binding. Cells were treated with ACHP (0–50 μM) for 4 h. Equal amounts (15 μg protein) of nuclear extracts were analyzed for NF-κB binding activity by EMSA using specific probe containing the NF-κB. Closed arrowhead indicates the location of the DNA-NF-κB complex.

in ATL-102 and MT-2 cells, no significant inhibition was observed in ED-40515 (−) cells. ICAM-1 was not expressed in ED-40515 (−) cells. When expression of CD25, as a negative control, was examined, ACHP treatment did not change the level of CD25 (data not shown).

Suppression of cell cycle progression and induction of apoptosis by ACHP

As shown in Figure 4a, ACHP reduced the fraction of cells at S phase in MT-2 and ED-40515 (−) cells, whereas no effect was observed in control Jurkat cells. These findings indicate that ACHP inhibits the growth of HTLV-1-infected T-cell lines in which NF-κB is constitutively activated. In Figure 4b, the number of cells undergoing apoptosis (annexinV-positive) was measured. In all HTLV-1-infected T-cell cell lines, apoptosis induction was remarkably observed at 50 μM, after 8 h treatment with ACHP. In addition, ACHP induced the cleavage of PARP in MT-2 and ED-40515 (−) cells (data not shown). We then examined the effects of ACHP on the growth of seven HTLV-1-infected T-cell lines and a control noninfected T-cell line (Jurkat). As shown in Figure 4c, ACHP inhibited the growth of these cells in a dose-dependent manner. Tax-active cell lines were more susceptible to ACHP than Tax-inactive cell lines and Jurkat (IC_{50} values in Tax-active cell lines, Tax-inactive cell lines or Jurkat were 3.1 ± 1.3 μM, 10.7 ± 1.7 μM and 23.6 μM, respectively), suggesting that the growth of Tax-active cells depends on NF-κB more than Tax-inactive cells. These observations are consistent with augmented NF-κB DNA binding and accelerated turn over of IκBα in Tax-active cells (Figures 1 and 2).

Growth inhibition and apoptosis induction of fresh ATL cells by ACHP

We then evaluated the effects of ACHP on the growth of fresh ATL cells obtained from four independent acute-type ATL patients. Peripheral blood mononuclear cells (PBMCs) contained greater than 90% leukemic cells. Control PBMCs were similarly obtained from four healthy individuals. As shown in Figure 5a, ACHP inhibited growth of fresh ATL cells. Fresh ATL leukemic cells were more susceptible to the ACHP-induced cell growth inhibition than control PBMCs from healthy individuals with IC_{50} values of 8.6 ± 1.1 and 55.7 ± 7.5 μM, respectively ($p < 0.01$). Compared with the data in Figure 4c with T-cell lines, the susceptibility of fresh ATL cells to ACHP was between Tax-active and inactive cells. However, healthy mononuclear cells were far more resistant to ACHP than Tax-inactive cells. These findings suggested that fresh ATL cells depend on NF-κB.

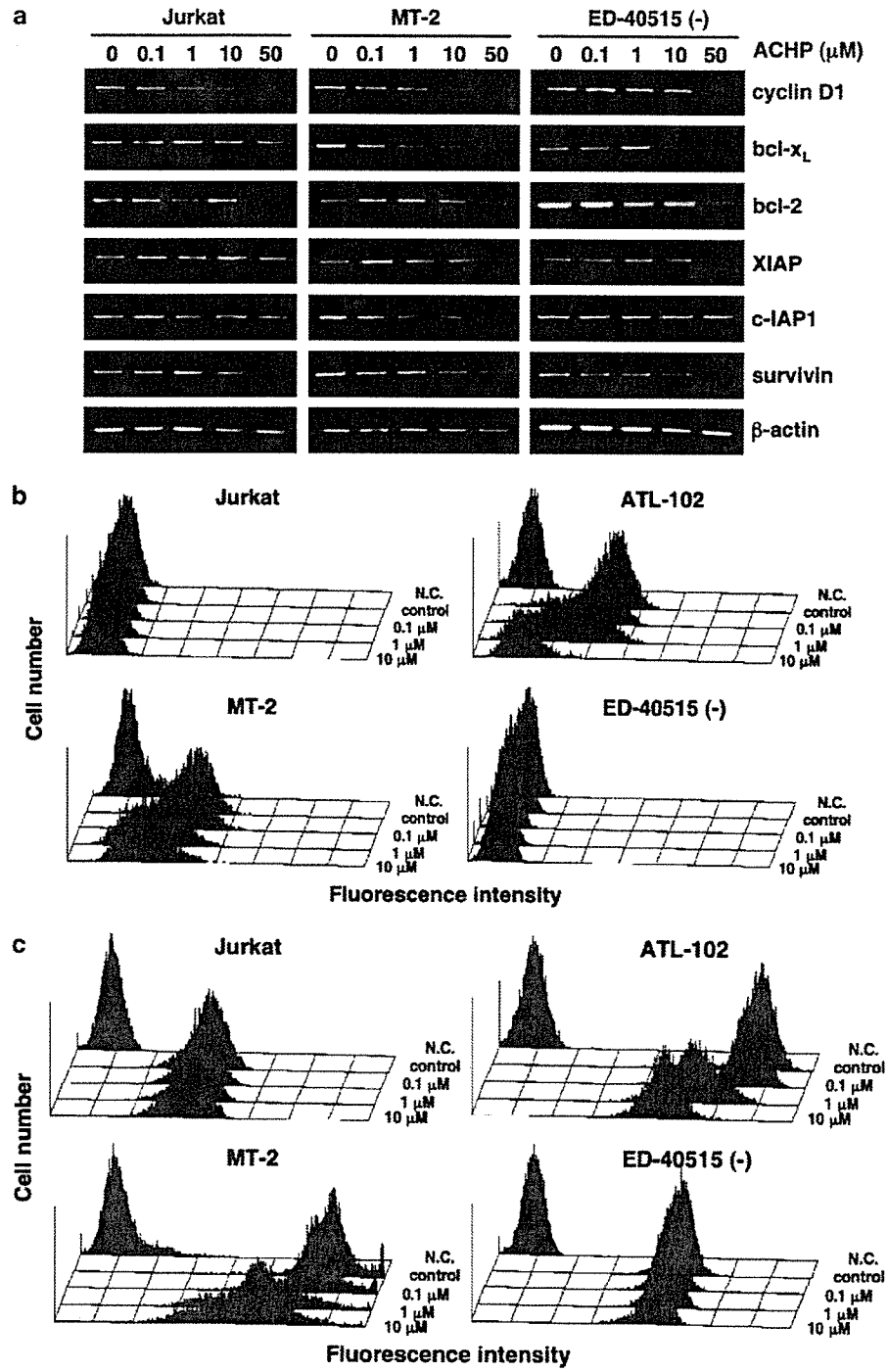

Figure 3 Inhibition of the NF-κB-dependent gene expression by ACHP. (**a**) Inhibition of gene expression by ACHP. The mRNA levels of various NF-κB target genes were examined by RT-PCR. Cells were treated with ACHP (0–50 μM) for 4 h, and total RNA were prepared and subjected to the determination of mRNA levels of *cyclin D1*, *bcl-xL*, *bcl-2*, *XIAP*, *c-IAP1*, *survivin* and *β-actin*. Each sample was subjected to PCR amplification for 35 cycles (*cyclin D1* in Jurkat cells) or 30 cycles (other genes). (**b**) and (**c**) Downregulation of ICAM-1 and VCAM-1 expression by ACHP. Surface expression of ICAM-1 (**b**) and VCAM-1 (**c**) was examined with Jurkat, ATL-102, MT-2 and ED-40515(−) cells in the absence (control) or presence of ACHP (0.1–10 μM) for 48 h by flowcytometry using specific antibodies. NC, negative control stained with isotype-matched IgG.

We then examined the levels of IκBα and p65 phosphorylation, as well as the NF-κB DNA binding, of fresh ATL cells and their susceptibility to ACHP-mediated apoptosis. As shown in Figure 5b, constitutive phosphorylation of p65 at Ser 536 and NF-κB DNA binding were observed and inhibited by ACHP (IC_{50} value: 0.6 μM), however, phosphorylation of IκBα at Ser 32 was not detected in fresh ATL cells. Identical results of protein phosphorylation were observed with other fresh ATL cells, whereas no constitutive phosphorylation of p65 and IκBα was observed with control PBMCs (data not shown). The flowcytometric analysis of fresh ATL cells (Figure 5c) revealed the appearance of prominent sub G_0/G_1 population suggesting the presence of cells undergoing apoptosis upon treatment with ACHP. Consistently, annexinV-positive cells were detected even

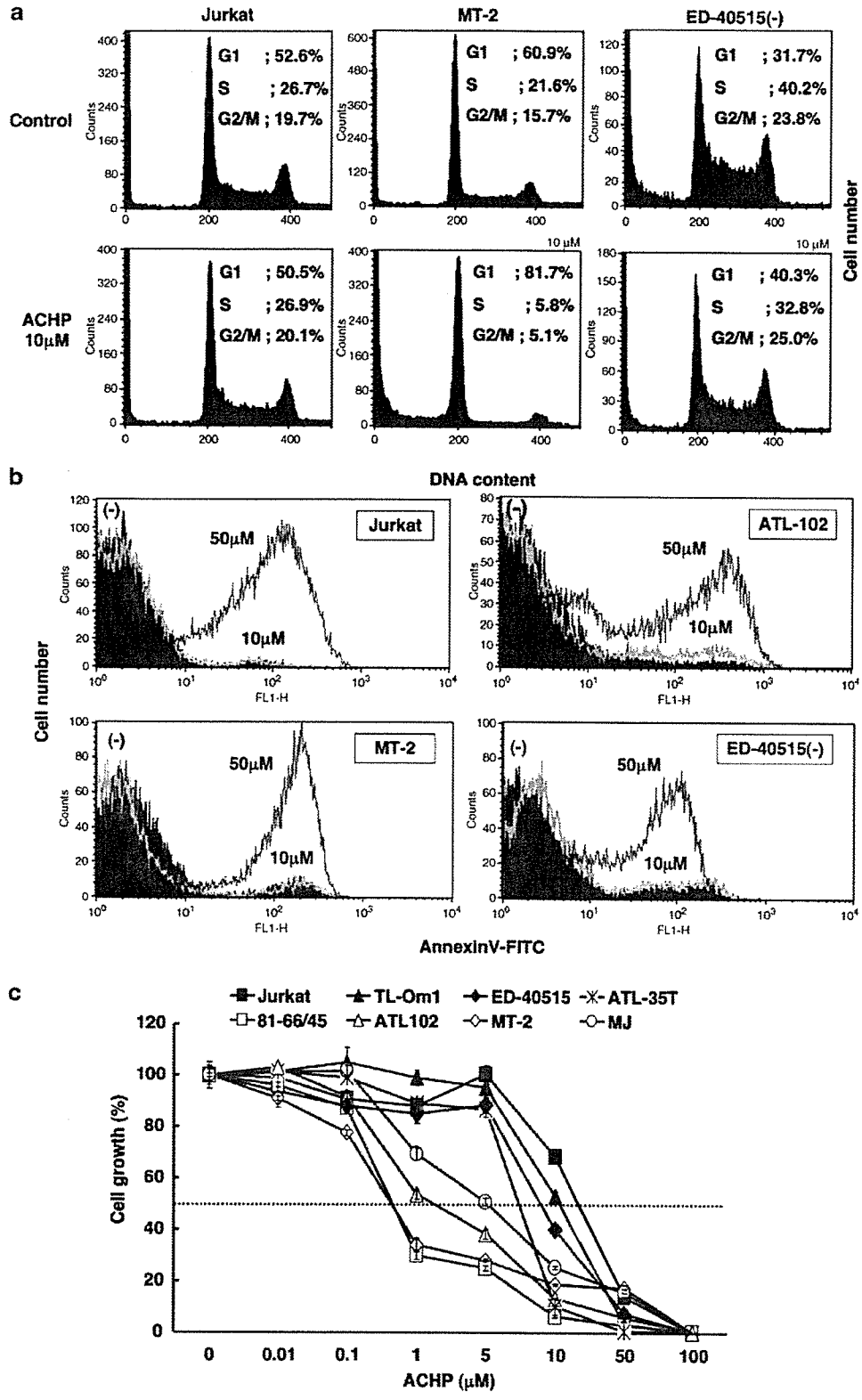

Figure 4 Growth inhibition, cell cycle arrest and induction of apoptosis by ACHP. (**a**) Inhibition of cell cycle progression. Cells were treated with or without ACHP (10 μM) for 24 h, stained with PI and subjected to the flowcytometric analysis. The fractions of each cell-cycle phase (%) are analyzed by CellQuest analysis program. Each experiment was repeated at least three times with reproducible results. The representative data are shown. (**b**) Induction of apoptosis. Cells were treated with ACHP (0, 10, 50 μM) for 8 h, stained with FITC-conjugated annexin V, and analyzed by flowcytometry. Closed areas indicate the intensities of nontreated control cells denoted as '(−)'. (**c**) Cell growth inhibition by ACHP. Cells were treated with ACHP for 3 days, before the cytotoxicity was evaluated by MTT assay. The results are indicated as percentage compared to the untreated control. These experiments were performed in triplicates and the mean values ± s.d. are shown.

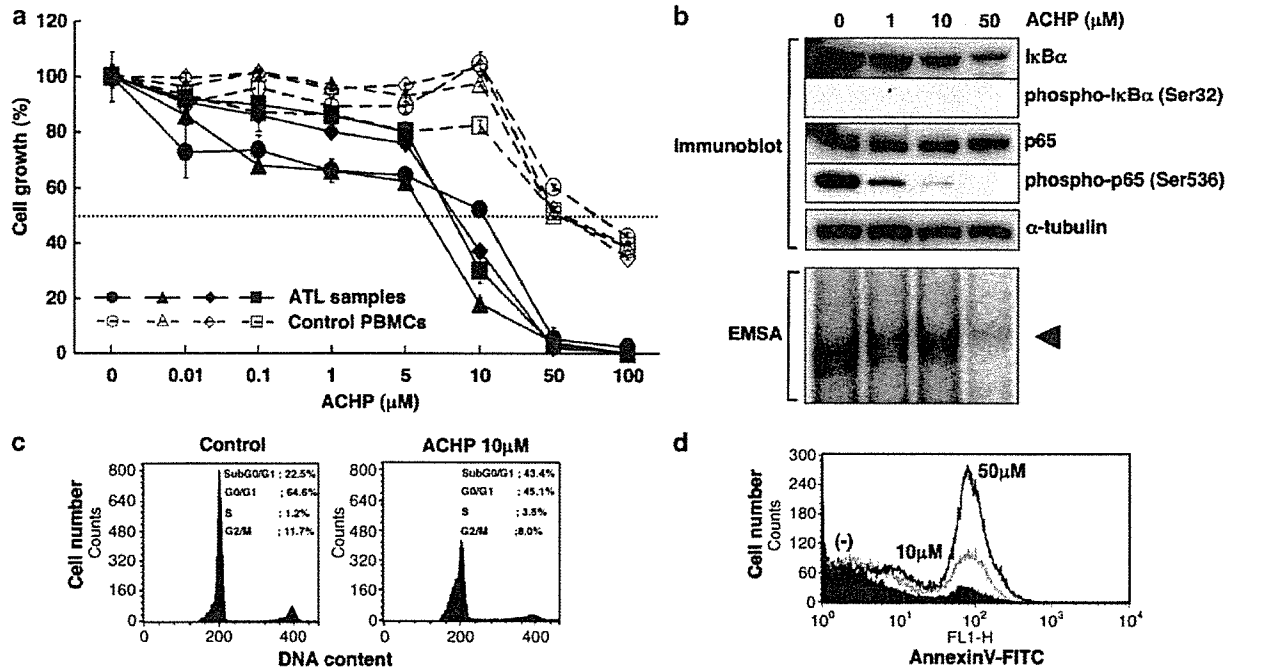

Figure 5 Growth inhibition and apoptosis induction of fresh ATL cells by ACHP. (**a**) Effects of ACHP on the cell growth of fresh ATL cells and control PBMCs. Four fresh ATL samples derived from acute-type ATL patients and four PBMCs derived from healthy donors were cultured in the absence of mitogen and treated with ACHP) for 3 days. The results are indicated as percentage compared to the untreated control. These experiments were performed in triplicates and the mean values ± s.d. are shown. (**b**) Dose-dependent inhibition of p65 phosphorylation and NF-κB DNA binding in fresh ATL cells. Fresh ATL cells were treated with ACHP for 6 h. Whole-cell extracts were subjected to immunoblotting analysis with the indicated antibodies, and nuclear extracts were subjected to EMSA. Closed arrowhead indicates the location of the DNA-NF-κB complex. (**c**) Cell cycle distribution analysis of fresh ATL cells upon treatment with ACHP. Fresh ATL cells were treated with or without ACHP (10 μM) for 24 h, stained with PI and subjected to the flowcytometric analysis. The fractions of each cell-cycle phase (%) are shown. Note the rapid appearance of subG$_0$/G$_1$ cells upon ACHP treatment. (**d**) Induction of apoptosis by ACHP. Fresh ATL cells were treated with ACHP (10 or 50 μM) for 8 h, stained with FITC-conjugated annexin V, and analyzed by flowcytometry. Closed areas indicate the intensities of nontreated control cells denoted as '(−)'.

with 10 μM of ACHP (Figure 5d). Thus, ACHP was effective in blocking the growth and inducing the apoptosis of ATL cells as well as HTLV-1-infected T-cell lines.

Discussion

In this study, we demonstrated that a novel IKK inhibitor, ACHP, efficiently inhibited NF-κB that is constitutively activated in ATL cell lines and fresh ATL cells. We also observed that it could block their growth by inducing apoptosis and cell cycle arrest. The constitutive activation of NF-κB has been reported in other neoplasms such as colorectal cancer, hepatocellular carcinoma, multiple myeloma and various forms of malignant lymphoma.[6,7,20] In these neoplasms, NF-κB was shown to be involved in tumorigenesis and disease progression by upregulating anti-apoptotic proteins, cell cycle regulators, and cell adhesion molecules. In fact, inhibitors of NF-κB such as Bay11-7082[13] showed antitumor effects. In addition, we have previously reported the growth inhibitory effect of ACHP on multiple myeloma cell lines and the synergism with conventional chemotherapeutic agents.[20]

We observed the growth inhibitory effect of ACHP especially in Tax-active HTLV-1-infected T-cell lines. In MT-2 cells, for example, the NF-κB DNA binding was prominent and was efficiently inhibited by ACHP (Figure 2d). On the other hand, in Tax-inactive cell lines such as ED-40515(−), phosphorylation of IκBα/p65 and NF-κB DNA binding was not inhibited until higher concentration (greater than 10 μM) of ACHP was used (Figure 2a and d). It was noted that the effective ACHP concentrations in blocking the phosphorylation and NF-κB DNA binding in these cell lines correlated with the extents of growth inhibition by ACHP (Figure 4c). Similar observations were reported by Mori *et al.*[13] where Tax-active HTLV-1-infected T-cell lines were more susceptible to the growth inhibitory effect of Bay 11-7082, another inhibitor of IKK, than Tax-inactive ATL cell lines.

The functional interaction between Tax and NF-κB activation pathway has been well investigated in previous studies by others.[16–18] In addition, constitutive activation of NF-κB is also reported in Tax-independent ATL cells[14,15] although the mechanism is not established yet. In these cells, it is postulated that the overexpression of TNFα or LTβ, which is often found in ATL patients,[22,31] could substitute the effects of Tax. We have demonstrated that LTβ receptor-mediated signaling specifically involves IKKα and induces p65 phosphorylation at Ser 536.[12] The constitutive phosphorylation of p65 at Ser 536 was evident in HTLV-1-infected T-cell lines irrespectively of the expression of functional Tax (Figure 1). In support of this possibility, Hironaka *et al.*[15] reported that dominant-negative IKKα mutant, but not dominant-negative IKKβ mutant, could inhibit the NF-κB activity in ATL-derived cell lines. Interestingly, we observed the NF-κB DNA binding associated with the constitutive p65 Ser 536 phosphorylation but not with the IκBα phosphorylation in fresh ATL samples (Figure 5b). In these cells, even lower concentrations of ACHP could induce apoptosis and cell growth arrest as compared with ATL cell lines (Figures 5c and d). These findings collectively suggest that the IKKα-mediated NF-κB activation pathway may play a crucial role in ATL.

In this study, we observed that various NF-κB target genes showed different susceptibility to the inhibitory effects of ACHP (Figure 3). For example, whereas expression of ICAM-1 and VCAM-1 was inhibited by the low dose of ACHP (Figure 3b and c), expression of anti-apoptotic genes, such as *bcl-XL, bcl-2, XIAP, c-IAP2* and *survivin*, required higher doses of ACHP (Figure 3a). It is possible that various NF-κB target genes are regulated by distinct NF-κB activation pathways. In this context, we found that IκBα phosphorylation, primarily catalyzed by IKKβ, was inhibited by low dose ACHP in HTLV-1-infected T cell lines (Figure 2). Thus, it appears that the ACHP-mediated inhibition of NF-κB target genes favors the canonical activation pathway. In addition, we found that ACHP could also induce apoptosis in Jurkat cells unexpectedly (Figure 2c) because no constitutive NF-κB activation was detected in these cells (Figures 1 and 2). In Jurkat cells the genetic defect of PTEN phosphatase is considered responsible for the cellular transformation.[32] The genetic defect of PTEN causes the constitutive Akt phosphorylation mediated by phosphatidylinositol-3 phosphate kinase (PI3K) and its inhibition by ACHP may have caused cell death in Jurkat. The constitutive Akt phosphorylation is also observed in the Tax-active cell lines (Figure 1a). Thus, it is possible that net effects of ACHP in inhibiting the growth of ATL cell lines may be through IKK-NF-κB and PI3K-Akt kinase pathways.

In conclusion, our results indicate the therapeutic efficacy of ACHP and its derivatives in the treatment of ATL by blocking the signal transduction pathway leading to constitutive activation of NF-κB, as well as Akt phosphorylation. Additionally, we observed the apparent differences in the NF-κB activation pathways involved in Tax-active, Tax-inactive, and most notably, fresh ATL cells and highlighted the role of IKKα in ATL leukemogenesis. Thus, ACHP and its derivatives could be feasible components of the novel anti-ATL chemotherapeutic regimen by sensitizing leukemic cells to the conventional cytotoxic agents.

Acknowledgements

We thank Drs M Matsuoka of Kyoto University for providing ED-40515(−) and TL-Om 1 cells, and Ms Ann Florence B Victoriano for language editing.We also thank Dr T Murata and KB Bacon for providing ACHP. This work is supported in part by grant-in-aids from the Ministry of Education, Culture, Sports, Science and Technology, and the Ministry of Health, Labor and Welfare of Japan.

References

1 Uchiyama T, Yodoi J, Sagawa K, Takatsuki K, Uchino H. Adult T-cell leukemia: clinical and hematologic features of 16 cases. *Blood* 1977; **50**: 481–492.
2 Poiesz BJ, Ruscetti FW, Gazdar AF, Bunn PA, Minna JD, Gallo RC. Detection and isolation of type C retrovirus particles from fresh and cultured lymphocytes of a patient with cutaneous T-cell lymphoma. *Proc Natl Acad Sci USA* 1980; **77**: 7415–7419.
3 Okamoto T, Ohno Y, Tsugane S, Watanabe S, Shimoyama M, Tajima K *et al.* Multi-step carcinogenesis model for adult T-cell leukemia. *Jpn J Cancer Res* 1989; **80**: 191–195.
4 Matsuoka M. Human T-cell leukemia virus type I and adult T-cell leukemia. *Oncogene* 2003; **22**: 5131–5140.
5 Hermine O, Dombret H, Poupon J, Arnulf B, Lefrere F, Rousselot P *et al.* Phase II trial of arsenic trioxide and alpha interferon in patients with relapsed/refractory adult T-cell leukemia/lymphoma. *Hematol J* 2004; **5**: 130–134.
6 Aggarwal BB. Nuclear factor-kappaB: the enemy within. *Cancer Cell* 2004; **6**: 203–208.
7 Pikarsky E, Porat RM, Stein I, Abramovitch R, Amit S, Kasem S *et al.* NF-kappaB functions as a tumour promoter in inflammation-associated cancer. *Nature* 2004; **431**: 461–466.
8 Okamoto T, Sakurada S, Yang JP, Merin JP. Regulation of NF-kappa B and disease control: identification of a novel serine kinase and thioredoxin as effectors for signal transduction pathway for NF-kappa B activation. *Curr Top Cell Regul* 1997; **35**: 149–161.
9 Collins T, Read MA, Neish AS, Whitley MZ, Thanos D, Maniatis T. Transcriptional regulation of endothelial cell adhesion molecules: NF-kappa B and cytokine-inducible enhancers. *Faseb J* 1995; **9**: 899–909.
10 Ghosh S, Karin M. Missing pieces in the NF-kappaB puzzle. *Cell* 2002; **109** (Suppl): S81–S96.
11 Pomerantz JL, Baltimore D. Two pathways to NF-kappaB. *Mol Cell* 2002; **10**: 693–695.
12 Jiang X, Takahashi N, Matsui N, Tetsuka T, Okamoto T. The NF-kappa B activation in lymphotoxin beta receptor signaling depends on the phosphorylation of p65 at serine 536. *J Biol Chem* 2003; **278**: 919–926.
13 Mori N, Yamada Y, Ikeda S, Yamasaki Y, Tsukasaki K, Tanaka Y *et al.* Bay 11-7082 inhibits transcription factor NF-kappaB and induces apoptosis of HTLV-I-infected T-cell lines and primary adult T-cell leukemia cells. *Blood* 2002; **100**: 1828–1834.
14 Mori N, Fujii M, Ikeda S, Yamada Y, Tomonaga M, Ballard DW *et al.* Constitutive activation of NF-kappaB in primary adult T-cell leukemia cells. *Blood* 1999; **93**: 2360–2368.
15 Hironaka N, Mochida K, Mori N, Maeda M, Yamamoto N, Yamaoka S. Tax-independent constitutive IkappaB kinase activation in adult T-cell leukemia cells. *Neoplasia* 2004; **6**: 266–278.
16 Suzuki T, Hirai H, Yoshida M. Tax protein of HTLV-1 interacts with the Rel homology domain of NF-kappa B p65 and c-Rel proteins bound to the NF-kappa B binding site and activates transcription. *Oncogene* 1994; **9**: 3099–3105.
17 Yin MJ, Christerson LB, Yamamoto Y, Kwak YT, Xu S, Mercurio F *et al.* HTLV-I Tax protein binds to MEKK1 to stimulate IkappaB kinase activity and NF-kappaB activation. *Cell* 1998; **93**: 875–884.
18 Xiao G, Cvijic ME, Fong A, Harhaj EW, Uhlik MT, Waterfield M *et al.* Retroviral oncoprotein Tax induces processing of NF-kappaB2/p100 in T cells: evidence for the involvement of IKKalpha. *EMBO J* 2001; **20**: 6805–6815.
19 Murata T, Shimada M, Sakakibara S, Yoshino T, Masuda T, Shintani T *et al.* Synthesis and structure-activity relationships of novel IKK-beta inhibitors. Part 3: Orally active anti-inflammatory agents. *Bioorg Med Chem Lett* 2004; **14**: 4019–4022.
20 Sanda T, Iida S, Ogura H, Asamitsu K, Murata T, Bacon KB *et al.* Growth inhibition of multiple myeloma cells by a novel IkappaB kinase inhibitor. *Clin Cancer Res* 2005; **11**: 1974–1982.
21 Iwatsuki K, Harada H, Motoki Y, Kaneko F, Jin F, Takigawa M. Diversity of immunobiological functions of T-cell lines established from patients with adult T-cell leukaemia. *Br J Dermatol* 1995; **133**: 861–867.
22 Tschachler E, Robert-Guroff M, Gallo RC, Reitz Jr MS. Human T-lymphotropic virus I-infected T cells constitutively express lymphotoxin in vitro. *Blood* 1989; **73**: 194–201.
23 Nakao Y, Koizumi T, Matsui T, Matsuda S, Nakagawa T, Katakami Y *et al.* Effect of 1 alpha,25-dihydroxyvitamin D3 on proliferation of activated T-cells and established human lymphotropic virus type I-positive T-cell lines. *J Natl Cancer Inst* 1987; **78**: 1079–1086.
24 Ishida T, Iida S, Akatsuka Y, Ishii T, Miyazaki M, Komatsu H *et al.* The CC chemokine receptor 4 as a novel specific molecular target for immunotherapy in adult T-Cell leukemia/lymphoma. *Clin Cancer Res* 2004; **10**: 7529–7539.
25 Dewan MZ, Terashima K, Taruishi M, Hasegawa H, Ito M, Tanaka Y *et al.* Rapid tumor formation of human T-cell leukemia virus type 1-infected cell lines in novel NOD-SCID/gammac(null) mice: suppression by an inhibitor against NF-kappaB. *J Virol* 2003; **77**: 5286–5294.
26 Zhong H, May MJ, Jimi E, Ghosh S. The phosphorylation status of nuclear NF-kappa B determines its association with CBP/p300 or HDAC-1. *Mol Cell* 2002; **9**: 625–636.
27 Nicot C, Mahieux R, Takemoto S, Franchini G. Bcl-X(L) is up-regulated by HTLV-I and HTLV-II in vitro and in ex vivo ATLL samples. *Blood* 2000; **96**: 275–281.

28 Kamihira S, Yamada Y, Hirakata Y, Tomonaga M, Sugahara K, Hayashi T *et al*. Aberrant expression of caspase cascade regulatory genes in adult T-cell leukaemia: survivin is an important determinant for prognosis. *Br J Haematol* 2001; **114**: 63–69.
29 Mori N, Fujii M, Hinz M, Nakayama K, Yamada Y, Ikeda S *et al*. Activation of cyclin D1 and D2 promoters by human T-cell leukemia virus type I tax protein is associated with IL-2-independent growth of T cells. *Int J Cancer* 2002; **99**: 378–385.
30 Ishikawa T, Imura A, Tanaka K, Shirane H, Okuma M, Uchiyama T. E-selectin and vascular cell adhesion molecule-1 mediate adult T-cell leukemia cell adhesion to endothelial cells. *Blood* 1993; **82**: 1590–1598.
31 Ishibashi K, Ishitsuka K, Chuman Y, Otsuka M, Kuwazuru Y, Iwahashi M *et al*. Tumor necrosis factor-beta in the serum of adult T-cell leukemia with hypercalcemia. *Blood* 1991; **77**: 2451–2455.
32 Wang X, Gjorloff-Wingren A, Saxena M, Pathan N, Reed JC, Mustelin T. The tumor suppressor PTEN regulates T cell survival and antigen receptor signaling by acting as a phosphatidylinositol 3-phosphatase. *J Immunol* 2000; **164**: 1934–1939.

Supplementary Information accompanies the paper on the Leukemia website (http://www.nature.com/leu)

Journal of General Virology (2006), 87, 1589–1593 DOI 10.1099/vir.0.81549-0

Short Communication

Suppression of human immunodeficiency virus type 1 replication by arginine deiminase of *Mycoplasma arginini*

Makoto Kubo,[1,2] Hironori Nishitsuji,[1] Kiyoshi Kurihara,[1] Takaya Hayashi,[1] Takao Masuda[1] and Mari Kannagi[1]

Correspondence
Mari Kannagi
kann.impt@tmd.ac.jp

[1]Department of Immunotherapeutics, Graduate School, Tokyo Medical and Dental University, 1-5-45 Yushima, Bunkyo-ku, Tokyo 113-8519, Japan

[2]Japanese Foundation for AIDS Prevention, Tokyo 105-0001, Japan

It was found previously that human immunodeficiency virus type 1 (HIV-1)-irrelevant CD8$^+$ cytotoxic T lymphocytes (CTLs) from uninfected donors suppressed HIV-1 replication in a cell-contact-dependent manner. However, one of these CTL lines (CTL-3) also significantly suppressed HIV-1 replication through its supernatant. Here, the suppressive fraction from CTL-3 supernatant was purified and analysed by mass spectrometry. A protein band specific for the suppressive fraction was identified as arginine deiminase from *Mycoplasma arginini*, which catalyses the hydrolysis of arginine to citrulline. Addition of L-arginine or the use of antibiotics against mycoplasma restored supernatant-mediated but not cell-contact-dependent suppression of HIV-1 replication by CTL-3, clearly indicating that arginine deiminase of *M. arginini* in the supernatants suppressed HIV-1 replication, which is independent of CD8$^+$ T-cell-mediated HIV-1 suppression via cell contact. Arginine deiminase is known to be a chemotherapeutic agent against arginine-requiring tumours and these results suggest that it also has potential application in antiviral therapy.

Received 21 September 2005
Accepted 31 January 2006

CD8$^+$ cells including human immunodeficiency virus type 1 (HIV-1)-specific cytotoxic T lymphocytes (CTLs) play important roles in controlling HIV-1 infection (Borrow *et al.*, 1994; McMichael & Rowland-Jones, 2001). It has been shown that CD8$^+$ cells of asymptomatic carriers produce an unknown CD8$^+$ T-cell antiviral factor that can suppress HIV-1 replication at a transcriptional level without causing cell death (Mackewicz *et al.*, 1995).

We have demonstrated previously that anti-HIV-1 activities of CD8$^+$ cells of asymptomatic carriers exhibit both major histocompatibility complex (MHC) I-restricted and -unrestricted suppression (Kannagi *et al.*, 1990; Ohashi *et al.*, 1999), and that HIV-1-irrelevant CD8$^+$ CTLs derived from uninfected donors also inhibit X4 and R5 HIV-1 replication (Liu *et al.*, 2003). Therefore, we hypothesized that MHC I-unrestricted suppression of HIV-1 replication might be a common property of CD8$^+$ CTLs, regardless of HIV-1 infection in the host. However, in our system, such CD8$^+$ cell-mediated suppression required direct contact between CD8$^+$ cells and infected cells.

Whilst investigating CD8$^+$ cell-mediated HIV-1 suppression, we established four allo-specific CD8$^+$ CTL lines, CTL-1 (Liu *et al.*, 2003), CTL-2, CTL-3 and CTL-4, from four uninfected healthy donors by stimulating peripheral blood mononuclear cells with mitomycin C (MMC)-treated Raji (Pulvertaft, 1964) cells in a long-term culture in the presence of recombinant human interleukin-2 (rhIL-2) as described previously (Liu *et al.*, 2003). These CTLs were not cytotoxic to autologous CD4$^+$ cells, but significantly suppressed HIV-1 replication in HIV-1-infected autologous CD4$^+$ cells when directly co-cultured.

Among these CTL lines, we found that culture supernatants of CTL-3 suppressed HIV-1 replication in addition to cell-mediated suppression. In the present study, we purified and identified the suppressive factor in the supernatant of CTL-3 by serial high-performance liquid chromatography (HPLC) and mass spectrometry.

Fig. 1 shows representative data of HIV-1 suppression by the established allo-specific CD8$^+$ CTL lines. CTLs from both the CTL-2 and CTL-3 lines markedly suppressed HIV-1 replication when directly co-cultured with HIV-1-infected autologous CD4$^+$ cells, whereas culture supernatants from CTL-3 but not CTL-2 suppressed HIV-1 replication (Fig. 1a). Culture supernatants of CTL-3 suppressed replication of both X4 HIV-1 strain NL4-3 (Adachi *et al.*, 1986) and R5 HIV-1 strain JR-CSF (Koyanagi *et al.*, 1987) (Fig. 1b). CTL-2 and CTL-3 culture supernatants did not alter the viability of CD4$^+$ T cells during 4 days of culture.

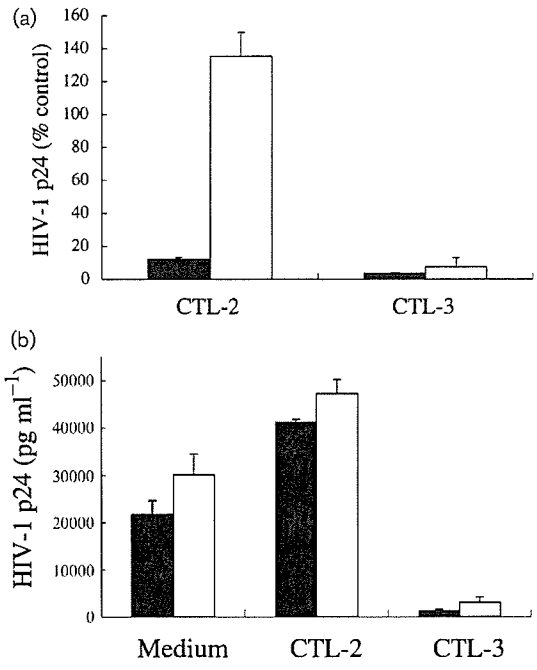

Fig. 1. Cell- and soluble factor-mediated suppression of HIV-1 replication by CD8$^+$ CTLs. (a) Cells (3×10^5 cells per well) (filled bar) or culture supernatants (50% vol.) (open bar) of two allo-specific CD8$^+$ CTL lines (CTL-2 and -3) established from two uninfected donors were co-cultured with phytohaemagglutinin-stimulated autologous CD4$^+$ cells (10^5 cells per well) infected with HIV-1 NL4-3 for 2 h *in vitro*. After culturing for 4 days, the amount of HIV-1 p24 in the supernatants was measured by ELISA (Cellular Products). The results indicate the amounts of HIV-1 p24 (%) compared with infected CD4$^+$ cells alone. The CTL culture supernatants used were prepared as fetal bovine serum (FBS) free and supplemented with 10% FBS for use. To prepare FBS-free supernatants, CTLs were washed 24 h after stimulation with MMC-treated Raji cells and the supernatants were harvested following another 48 h of culture at a concentration of 5×10^6 cells ml^{-1} in FBS-free RPMI 1640 in the presence of 50 U rhIL-2 ml^{-1}. The supernatants were passed through 0·22 μm filters before use. (b) Similarly prepared culture supernatants of CTL-2 and -3 were added at 50% concentrations into acutely HIV-1 NL4-3 (filled bar)- or JR-CSF (open bar)-infected CD4$^+$ cell cultures for 4 days and the amount of HIV-1 p24 in the supernatants was measured by ELISA. The results indicate the mean ± SD of duplicate wells. Similar results were obtained when CTL supernatants prepared in the presence of FBS were used. The viability of CD4$^+$ T cells after 4 days of culture with medium or with CTL-2 and CTL-3 culture supernatants was 95·37 ± 0·13, 97·84 ± 0·15 and 98·64 ± 0·08%, respectively, as determined by flow cytometry following staining with fluorescein isothiocyanate–annexin V and 7-aminoactinomycin D.

In order to purify the suppressive factor(s), first we separated the CTL-3 culture supernatant on an anion-exchange UNO-Q1 column (Bio-Rad) with a linear gradient from 0 to 1·0 M NaCl in 10 mM potassium phosphate buffer (pH 7·0) using HPLC (Fig. 2a). The HIV-1-suppressive

Fig. 2. Purification and identification of an HIV-1-suppressive factor in CTL-3 culture supernatants by HPLC. (a) FBS-free culture supernatants of CTL-3 prepared as described in Fig. 1 legend were concentrated with Amicon Ultra-4 (Millipore), applied to an anion-exchange column (UNO-Q1; Bio-Rad) and eluted with a linear gradient (0–1·0 M NaCl) in 10 mM potassium phosphate buffer at a flow rate of 1 ml min^{-1} using an HPLC system (BioCAD; Applied Biosystems). Protein peaks, conductivity and fraction numbers are indicated. (b) Each fraction was dialysed against PBS, cleared through a 0·22 μm filter, supplemented with 10% FBS and added to an HIV-1 NL4-3-infected CD4$^+$ cell culture at a concentration of 50%. The same volume of PBS with 10% FBS was used as a control (open bar). After 4 days of incubation, the amount of HIV-1 p24 in the culture supernatants was measured by ELISA. The results indicate the mean ± SD of duplicate wells. (c) Fraction #26 separated by anion-exchange HPLC was further subjected to gel filtration on a TSK gel 2000 column (Tosoh) using HPLC at a flow rate of 0·5 ml min^{-1} in PBS. Protein peaks, conductivity and fraction numbers are indicated. (d) Each gel-filtrated HPLC fraction was evaluated for HIV-1-suppressive activity as described in (b). (e) Fractions #26-13, -14 and -15, separated as described in (c) from two independently prepared samples, were subjected to 7·5% SDS-PAGE at a constant current of 24 mA per gel for 5 h. The proteins were visualized by silver staining (ProteoSilver Plus Silver Stain kit; Sigma-Aldrich). Similarly purified fractions from culture supernatants containing MMC-treated Raji cells alone served as controls. The arrow at 45 kDa indicates the bands specific for the fractions with HIV-1-suppressive activity. (f) The protein band at 45 kDa was excised from the SDS-polyacrylamide gel, digested with lysyl endopeptidase and subjected to MALDI-TOF-MS using an Ultraflex TOF/TOF mass spectrometer (Bruker Daltonics) as described previously (Yamagata *et al.*, 2002). The MS spectrum of this protein as shown was analysed by MASCOT software (Matrix Science) with the NCBInr database and identified as arginine deiminase from *M. arginini*.

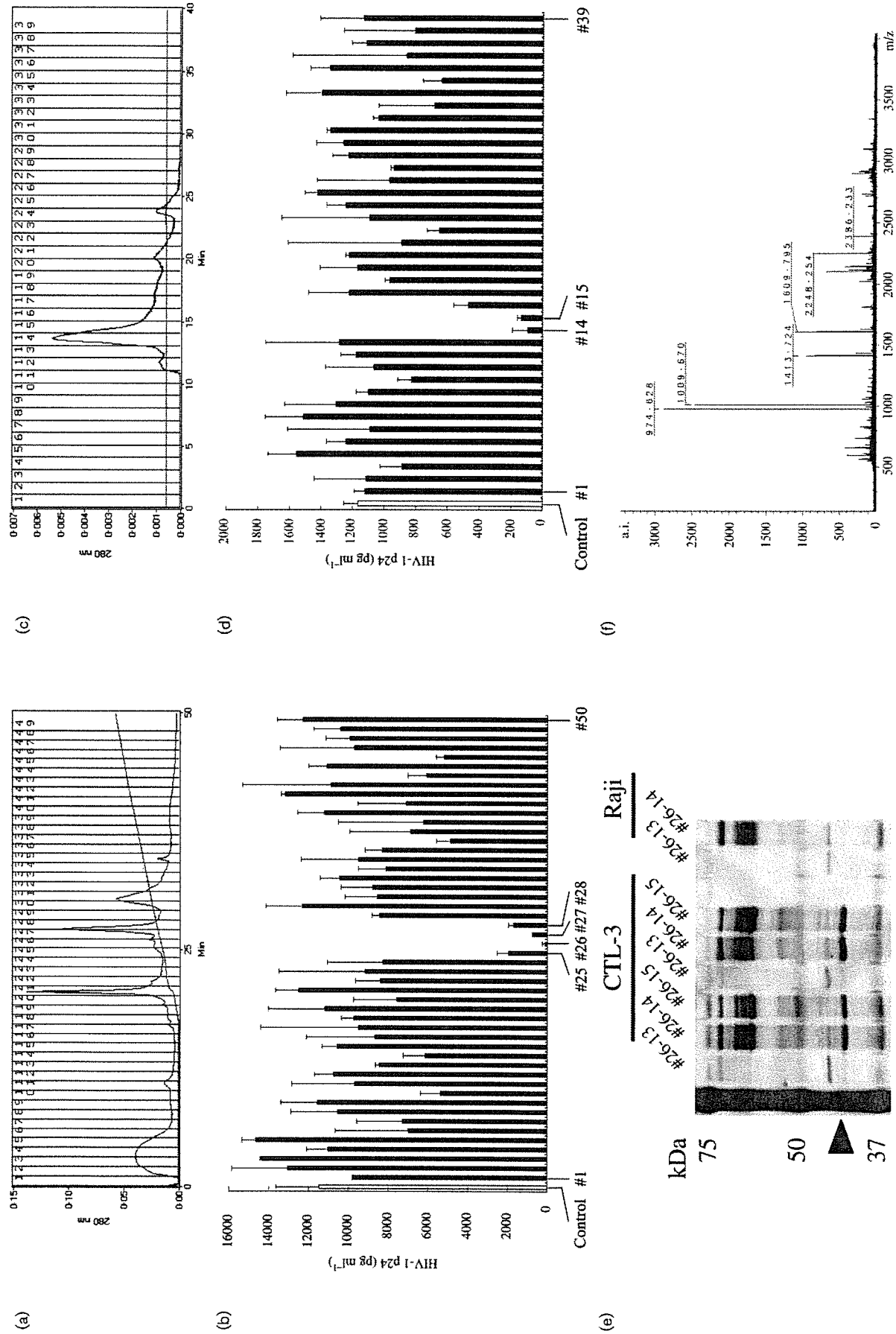
(a)
280 nm
Min
(b)
HIV-1 p24 (pg ml⁻¹)
Control #1
#25 #26 #27 #28
#50
(c)
280 nm
Min
(d)
HIV-1 p24 (pg ml⁻¹)
Control #1
#14 #15
#39
(e)
CTL-3
#26-13
#26-14
#26-15
#26-13
#26-14
#26-15
Raji
#26-13
#26-14
kDa
75
50
37
(f)
a.u.
m/z
974.1 - 1026
1009.1 - 1079
1413.3 - 1724
1698.3 - 1795
2248.2 - 2543
2386.2 - 2543

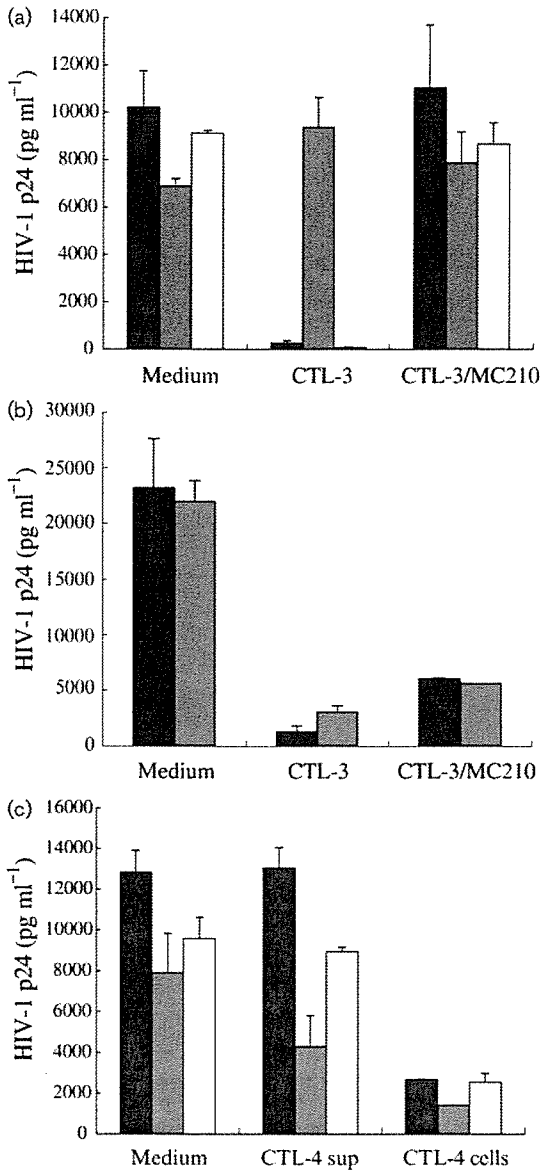

Fig. 3. L-Arginine and MC210 restore the supernatant- but not cell-mediated suppression of HIV-1 replication by CTL-3. (a) Culture supernatants from CTL-3 cells and CTL-3 cells treated with an antibiotic against mycoplasma (MC210; Dainippon Pharmaceutical) for 2 weeks (CTL-3/MC210) were added to an acutely HIV-1 NL4-3-infected CD4$^+$ cell culture in the absence (filled bar) or presence of 10 mM L-arginine (shaded bar) or L-glycine (open bar). HIV-1 p24 concentration in the supernatants was measured by ELISA 4 days after infection. (b) CTL-3 or CTL-3/MC210 cells were directly co-cultured with phytohaemagglutinin-stimulated autologous CD4$^+$ cells (10^5 cells per well) acutely infected with HIV-1 NL4-3 at a CTL : CD4$^+$ cell ratio of 3 in the absence (filled bar) or presence (shaded bar) of 10 mM L-arginine for 4 days. The amount of HIV-1 p24 in the supernatants was measured by ELISA. (c) Culture supernatants or cells from another mycoplasma-free CTL line (CTL-4) were co-cultured with HIV-1 NL4-3-infected autologous CD4$^+$ cells in the absence (filled bar) or presence of 10 mM L-arginine (shaded bar) or L-glycine (open bar) for 4 days and HIV-1 p24 concentration in the supernatants was measured. The results indicate the mean ± SD of duplicate wells.

activity of each fraction (1 ml) was evaluated following direct co-culture with CD4$^+$ cells infected with HIV-1 NL4-3. As shown in Fig. 2(b), fractions #25 to #28 of anion-exchange HPLC markedly suppressed the replication of HIV-1. The suppressive activity peaked at fraction #26 in more than three independent experiments.

Fraction #26 was subsequently separated by gel filtration on a TSK gel 2000 column (Tosoh) using HPLC (Fig. 2c). The resulting fractions, #14 and #15 (designated #26-14 and #26-15, respectively, hereafter) markedly suppressed HIV-1 replication (Fig. 2d).

Next, HIV-1-suppressive fractions #26-14 and -15, serially purified by anion-exchange and gel-filtrated HPLC from CTL-3 supernatants, were resolved by 7·5 % SDS-PAGE. As a control, similarly purified fractions from culture supernatants of MMC-treated Raji cells were used. As shown in Fig. 2(e), silver staining showed protein bands at 45 kDa that were observed only in #26-14 and -15, and not in the control fractions. The 45 kDa protein bands were cut from a separately prepared negatively stained gel (Wako) and subjected to matrix-assisted laser desorption/ionization time-of-flight mass spectrometry (MALDI-TOF-MS).

Fig. 2(f) demonstrates the MS spectrum of peptides extracted from the 45 kDa band after digestion with lysyl endopeptidase, obtained using an Ultraflex TOF/TOF mass spectrometer (Kristensen *et al.*, 2000; Yamagata *et al.*, 2002). Several peaks were analysed further by MS/MS (data not shown). Computer analysis of the MS and MS/MS spectra using MASCOT software (Matrix Science) with the NCBInr database identified the protein as arginine deiminase from *Mycoplasma arginini*. The results strongly indicated that the CTL-3 cells had been contaminated by *M. arginini*, although growth of the CTL-3 cells was not affected.

Finally, we examined whether the suppressive effects of CTL-3 supernatants on HIV-1 replication were attributed to arginine deiminase. Arginine deiminase is a mycoplasma enzyme that catalyses the imine hydrolysis of arginine to citrulline and ammonia. When L-arginine (10 mM) was added to an HIV-1-infected CD4$^+$ cell culture together with CTL-3 culture supernatant, the suppression of HIV-1 replication was almost completely restored (Fig. 3a), clearly indicating that the suppressive effects were mediated mostly by arginine deiminase. L-Glysine (10 mM) as a control showed no effect. In addition, treatment of the CTL-3 culture with antibiotic MC210 against mycoplasma for approximately 2 weeks abolished the HIV-1-suppressive activity of the culture supernatants (Fig. 3a).

In contrast, CTL-3 and MC210-treated CTL-3 cells continued to show significant levels of suppressive effects on HIV-1 replication when directly co-cultured with HIV-1-infected autologous CD4$^+$ cells in the presence of L-arginine (Fig. 3b), indicating that cell-mediated suppression of HIV-1 replication was not attributed to arginine deiminase. The presence of cell-mediated but not supernatant-mediated

suppressive effects on HIV-1 replication was also confirmed by using another mycoplasma-free $CD8^+$ CTL line (CTL-4) (Fig. 3c).

Our results clearly indicate that arginine deiminase from *M. arginini* suppresses HIV-1 replication in $CD4^+$ cells *in vitro*. Although arginine is a non-essential amino acid for humans and mice, some cancers have an elevated requirement for arginine. Arginine deiminase inhibits the growth of arginine-requiring tumours such as human melanomas and hepatocellular carcinoma *in vitro* and *in vivo*, suggesting its potential use as a chemotherapeutic reagent (Curley *et al.*, 2003; Ensor *et al.*, 2002).

Mycoplasma contamination of HIV-1-infected culture causes various effects *in vitro*, such as enhancement of the cytopathic effects associated with HIV-1 replication (Lo *et al.*, 1991), inhibition of CD4 expression and gp120 binding (O'Toole & Lowdell, 1990) and apparent reduction of reverse transcriptase activity, probably due to nuclease activity (el-Farrash *et al.*, 1994; Shang *et al.*, 1995; Vasudevachari *et al.*, 1990). *Mycoplasma penetrans* isolated from HIV-1-infected individuals potentially activates T lymphocytes and HIV-1 replication, suggesting its contribution to disease progression (Sasaki *et al.*, 1995). This variety of effects might partly be due to the variety of *Mycoplasma* species.

In the present study, we identified arginine deiminase as a suppressive factor of HIV-1 replication. Although we found it in a $CD8^+$ CTL line possessing HIV-1-suppressive activity, only supernatant-mediated and not cell-contact-dependent suppression of HIV-1 was attributed to arginine deiminase. The precise mechanisms of arginine deiminase-mediated inhibition of the HIV-1 replication cycle remain to be clarified.

Acknowledgements

We thank ProPhoenix Co. Ltd (Higashi-Hiroshima, Japan) for analysis of protein bands by MALDI-TOF-MS. This work was supported by grants from the Ministry of Health, Welfare and Labor, Japan.

References

Adachi, A., Gendelman, H. E., Koenig, S., Folks, T., Willey, R., Rabson, A. & Martin, M. A. (1986). Production of acquired immunodeficiency syndrome-associated retrovirus in human and nonhuman cells transfected with an infectious molecular clone. *J Virol* **59**, 284–291.

Borrow, P., Lewicki, H., Hahn, B. H., Shaw, G. M. & Oldstone, M. B. (1994). Virus-specific $CD8^+$ cytotoxic T-lymphocyte activity associated with control of viremia in primary human immunodeficiency virus type 1 infection. *J Virol* **68**, 6103–6110.

Curley, S. A., Bomalaski, J. S., Ensor, C. M., Holtsberg, F. W. & Clark, M. A. (2003). Regression of hepatocellular cancer in a patient treated with arginine deiminase. *Hepatogastroenterology* **50**, 1214–1216.

el-Farrash, M. A., Kannagi, M., Kuroda, M. J., Yoshida, T. & Harada, S. (1994). The mycoplasma-related inhibitor of HIV-1 reverse transcriptase has a DNase activity and is present in the particle-free supernatants of contaminated cultures. *J Virol Methods* **47**, 73–82.

Ensor, C. M., Holtsberg, F. W., Bomalaski, J. S. & Clark, M. A. (2002). Pegylated arginine deiminase (ADI-SS $PEG_{20,000\ mw}$) inhibits human melanomas and hepatocellular carcinomas *in vitro* and *in vivo*. *Cancer Res* **62**, 5443–5450.

Kannagi, M., Masuda, T., Hattori, T., Kanoh, T., Nasu, K., Yamamoto, N. & Harada, S. (1990). Interference with human immunodeficiency virus (HIV) replication by $CD8^+$ T cells in peripheral blood leukocytes of asymptomatic HIV carriers in vitro. *J Virol* **64**, 3399–3406.

Koyanagi, Y., Miles, S., Mitsuyasu, R. T., Merrill, J. E., Vinters, H. V. & Chen, I. S. (1987). Dual infection of the central nervous system by AIDS viruses with distinct cellular tropisms. *Science* **236**, 819–822.

Kristensen, D. B., Imamura, K., Miyamoto, Y. & Yoshizato, K. (2000). Mass spectrometric approaches for the characterization of proteins on a hybrid quadrupole time-of-flight (Q-TOF) mass spectrometer. *Electrophoresis* **21**, 430–439.

Liu, H., Ohashi, T., Masuda, T., Zhou, X., Kubo, M. & Kannagi, M. (2003). Suppression of HIV-1 replication by HIV-1-irrelevant $CD8^+$ cytotoxic T lymphocytes resulting in preservation of persistently HIV-1-infected cells in vitro. *Viral Immunol* **16**, 381–393.

Lo, S. C., Tsai, S., Benish, J. R., Shih, J. W., Wear, D. J. & Wong, D. M. (1991). Enhancement of HIV-1 cytocidal effects in $CD4^+$ lymphocytes by the AIDS-associated mycoplasma. *Science* **251**, 1074–1076.

Mackewicz, C. E., Blackbourn, D. J. & Levy, J. A. (1995). $CD8^+$ T cells suppress human immunodeficiency virus replication by inhibiting viral transcription. *Proc Natl Acad Sci U S A* **92**, 2308–2312.

McMichael, A. J. & Rowland-Jones, S. L. (2001). Cellular immune responses to HIV. *Nature* **410**, 980–987.

Ohashi, T., Kubo, M., Kato, H., Iwamoto, A., Takahashi, H., Fujii, M. & Kannagi, M. (1999). Role of class I major histocompatibility complex-restricted and -unrestricted suppression of human immunodeficiency virus type 1 replication by $CD8^+$ T lymphocytes. *J Gen Virol* **80**, 209–216.

O'Toole, C. & Lowdell, M. (1990). Infection of human T cells with mycoplasma, inhibition of CD4 expression and HIV-1 gp120 glycoprotein binding, and infectivity. *Lancet* **336**, 1067.

Pulvertaft, J. V. (1964). Cytology of Burkitt's tumour (African Lymphoma). *Lancet* **283**, 238–240.

Sasaki, Y., Blanchard, A., Watson, H. L., Garcia, S., Dulioust, A., Montagnier, L. & Gougeon, M. L. (1995). In vitro influence of *Mycoplasma penetrans* on activation of peripheral T lymphocytes from healthy donors or human immunodeficiency virus-infected individuals. *Infect Immun* **63**, 4277–4283.

Shang, H., Miyakawa, Y., Sasaki, T., Nakashima, H. & Ito, M. (1995). Suppression of HIV-1 reverse transcriptase activity by culture supernatants of mycoplasmas. *Microbiol Immunol* **39**, 987–993.

Vasudevachari, M. B., Mast, T. C. & Salzman, N. P. (1990). Suppression of HIV-1 reverse transcriptase activity by mycoplasma contamination of cell cultures. *AIDS Res Hum Retroviruses* **6**, 411–416.

Yamagata, A., Kristensen, D. B., Takeda, Y., Miyamoto, Y., Okada, K., Inamatsu, M. & Yoshizato, K. (2002). Mapping of phosphorylated proteins on two-dimensional polyacrylamide gels using protein phosphatase. *Proteomics* **2**, 1267–1276.

JOURNAL OF VIROLOGY, June 2006, p. 5670–5677 Vol. 80, No. 12
0022-538X/06/$08.00+0 doi:10.1128/JVI.02471-05

Identification of a Novel Human Immunodeficiency Virus Type 1 Integrase Interactor, Gemin2, That Facilitates Efficient Viral cDNA Synthesis In Vivo

Seiji Hamamoto,[1,2]† Hironori Nishitsuji,[1]† Teruo Amagasa,[2] Mari Kannagi,[1] and Takao Masuda[1]*

Department of Immunotherapeutics, Graduate School of Medicine and Dentistry, Tokyo Medical and Dental University, 1-5-45 Yushima, Bunkyo-ku, Tokyo 113-8519, Japan,[1] and Department of Maxillofacial Surgery, Graduate School of Medicine and Dentistry, Tokyo Medical and Dental University, 1-5-45 Yushima, Bunkyo-ku, Tokyo 113-8549, Japan[2]

Received 23 November 2005/Accepted 27 March 2006

Retroviral integrase (IN) catalyzes the integration of viral cDNA into a host chromosome. Additional roles have been suggested for IN, including uncoating, reverse transcription, and nuclear import of the human immunodeficiency virus type 1 (HIV-1) genome. However, the underlying mechanism is largely unknown. Here, using a yeast two-hybrid system, we identified a survival motor neuron (SMN)-interacting protein 1 (Gemin2) that binds to HIV-1 IN. Reduction of Gemin2 with small interfering RNA duplexes (siGemin2) dramatically reduced HIV-1 infection in human primary monocyte-derived macrophages and also reduced viral cDNA synthesis. In contrast, siGemin2 did not affect HIV-1 expression from the integrated proviral DNA. Although Gemin2 was undetectable in cell-free viral particles, coimmunoprecipitation experiments using FLAG-tagged Gemin2 strongly suggested that Gemin2 interacts with the incoming viral genome through IN. Further experiments reducing SMN or other SMN-interacting proteins suggested that Gemin2 might act on HIV-1 either alone or with unknown proteins to facilitate efficient viral cDNA synthesis soon after infection. Thus, we provide the evidence for a novel host protein that binds to HIV-1 IN and facilitates viral cDNA synthesis and subsequent steps that precede integration in vivo.

When a cell is infected with a retrovirus, the viral genome is subjected to several processes that include uncoating, reverse transcription of the viral genomic RNA into a cDNA copy by use of reverse transcriptase (RT), transport of this cDNA into the nucleus, and integration of the cDNA into the host chromosome. These early events are mediated through the interactions of several viral proteins and host factors with the viral genome, often referred as the reverse transcription complex or preintegration complex (4, 8, 16). The integration of a viral cDNA copy into a host cell chromosome is accomplished by integrase (IN) (24).

Mutational analyses of human immunodeficiency virus type 1 (HIV-1) IN have suggested putative roles for IN at steps prior to integration, such as uncoating (25, 29, 32), reverse transcription (11, 29, 37, 39), and nuclear import of viral cDNA (5, 20, 37). However, the mechanisms for these pleiotropic effects of IN mutations are largely unknown. Several cellular proteins, including integrase interactor 1 (23, 41) and human lens epithelium-derived growth factor-transcription coactivator p75 (27, 28), have been reported to interact directly with HIV-1 IN for chromosomal targeting of HIV-1 IN. Meanwhile, there has been increasing evidence of physical interactions between IN and RT during reverse transcription of HIV-1 (12, 19, 42), murine leukemia virus (MLV) (13), and *Saccharomyces cerevisiae* retrovirus-like element Ty3 (33). The results of an endogenous RT assay using purified HIV-1 virus particles also suggested that a cellular cofactor(s) might be required to complete reverse transcription in vivo (29).

In this study, we identified a novel host protein that binds to HIV-1 integrase and plays a critical role in HIV-1 infection in vivo. Survival motor neuron (SMN)-interacting protein 1 (Gemin2) (26) is a member of the SMN complex that mediates the assembly of spliceosomal small nuclear ribonucleoproteins (snRNPs) (3, 15, 21, 26, 30). Our results suggest that Gemin2 interacts with IN in the incoming virus genome complex and is essential for HIV-1 infection and viral cDNA synthesis and subsequent steps that proceed to integration.

MATERIALS AND METHODS

Plasmids. DNA fragments of the full-length HIV-1 IN were amplified by PCR from the HIV-1 pNL4-3lucΔenv vector by use of the oligonucleotide sense primer GBT9IN-1R (5′-CCGGAATTCTTTTTAGATGGAATA-3′) and the oligonucleotide antisense primer GBT9INenBH (5′-ACGGATCCTTAATCCT CATCCTG-3′). In the pNL4-3lucΔenv vector, the *env* gene has been deleted and the *nef* gene has been replaced with the firefly luciferase (Luc) gene (29). The amplified PCR products were digested with the restriction enzymes EcoRI and BamHI and ligated into the pGBT9 vector (BD Biosciences, San Jose, CA) (pGBT-IN). The pGBT9 vector constructs with truncated forms of IN (pGBT-ΔN-IN, pGBT-ΔN/ΔC-IN, and pGBT-INΔC) were similarly prepared using the following primer pairs: for pGBT-ΔN-IN, the sense primer GBT9IN50R (5′-CCGGAA TTCCATGGACAAGTAGAC-3′) and the antisense primer GBT9INenBH (corresponding to IN amino acid positions 51 to 288); for pGBT-ΔN/ΔC-IN, the sense primer GBT9IN50R and the antisense primer GBT9IN210BH (5′-ACGG ATCCAGTTTGTATGTCTGT-3′) (corresponding to IN amino acid positions 51 to 210); and for pGBT-IN-ΔC, the sense primer GBT9IN-1R and the antisense primer GBT9IN210BH (corresponding to IN amino acid positions 1 to 210). The pGAD-GH vector containing a HeLa cDNA library pretransformed into yeast strain Y187 was purchased from BD Biosciences. For preparation of a lentiviral vector expressing FLAG-tagged Gemin2, an EcoRI-XbaI fragment

* Corresponding author. Mailing address: Department of Immunotherapeutics, Graduate School, Tokyo Medical and Dental University, 1-5-45 Yushima, Bunkyo-ku, Tokyo 113-8519, Japan. Phone: 81-3-5803-5799. Fax: 81-3-5803-0235. E-mail: tmasu.impt@tmd.ac.jp.
† S.H. and H.N. contributed equally to this work.

from pTRE-FLAG-Gemin2 (34) (kindly provided by G. Dreyfuss, University of Pennsylvania) was ligated into the pCSII-CMV-MCS vector (31) (kindly provided by H. Miyoshi, RIKEN Tsukuba Institute) or the pEF6/V5-HisA expression vector (Invitrogen). For construction of an small interfering RNA (siRNA)-resistant Gemin2 expression vector, silent point mutations were introduced into the target sequences of siGemin2#372 by use of mutagenic oligonucleotides (5′-CCTCCCTTGCTTAGCATCGTAAGCAGAATGAATC-3′).

Yeast mating and cDNA isolation. The pGBT-IN plasmid was transformed into yeast strain AH109, and yeast mating was performed according to the manufacturer's instructions (BD Biosciences). Positive transformants were verified for beta-galactosidase activity as described in the instructions.

Cells. HeLa and 293T cells were maintained in Dulbecco's modified Eagle's medium (DMEM; MP Biomedicals Inc., Irvine, CA) supplemented with 10% (vol/vol) heat-inactivated fetal bovine serum (FBS) (Invitrogen, Carlsbad, CA), 2 μg/ml sodium hydrogen carbonate (Wako, Osaka, Japan), 0.88 μg/ml tissue culture powdered DMEM amino acid and vitamin medium (Nissui Pharmaceutical Co., Ltd., Tokyo, Japan), 100 units/ml penicillin G, and 100 μg/ml streptomycin sulfate. Human peripheral blood mononuclear cells were isolated from HIV-1-seronegative healthy individuals by use of Ficoll-Paque Plus (Amersham Pharmacia Biotech Inc., Tokyo, Japan) density centrifugation. Human monocyte-derived macrophages (MDMs) were subsequently isolated from the peripheral blood mononuclear cells and cultured with RPMI 1640 (GIBCO, Invitrogen) supplemented with 5% human AB serum (Nippon Bio-supply Center, Tokyo, Japan) as described previously (37).

Construction of siRNAs. An siRNA duplex (small interfering green fluorescent protein [siGFP]) targeting the sequence 5′-AAGGUGCUCUGAAGUGA GGCU-3′ in the open reading frame of human Gemin2 (siGemin2) and a control double-stranded RNA targeting the 5′-CGGCAAGCUGACCCUGAA GUUC-3′ sequence in siGFP were purchased from QIAGEN K. K. (Tokyo, Japan). The targeting sequences of Gemin2 for the chemically modified synthetic siRNA duplexes (Stealth RNAi) purchased from Invitrogen were as follows: for siGemin2#372, 5′-CCU UGC UUA GUA UUG UUA GCA GAA U-3′; for siGemin2#373, 5′-GGA UAG CAA AGA UGA UGA GAG GGU U-3′; for siGemin2#374, 5′-UGA CCA ACG UGA UUU AGC UGA UGA G-3′; for siGemin2#375,5′-CAA GAA GGU GCU CUG AAG UGA GGC U-3′; for siGemin2#mm375, 5′-CAA GGA CGU UCU AAG GUG GAG AGC U-3′; for small interfering SMN#271 (siSMN#271), 5′-UAC UGG CUA UUA UAU GGG UUU CAG A-3′; for siSMN#272, 5′-CCA AAA GAA GAA UAC UGC AGC UUC C-3′; for siGemin3#430, 5′-CCA GUG AUC CAA GUC UCA UAG GUU U-3′; for siGemin3#431, 5′-GCU GCC GCU UCU CAU UCA UAU UAU U-3′; for siGemin3#432, 5′-GCU GUU GGA UCU CCU GGC AGA AUU A-3′; for siGemin4#354, 5′-GAA CUG CCU GAU GAG UCC CGU GAA A-3′; for siGemin4#355, 5′-AGG GAU UCC AGU GGC UGC UCU UCU U-3′; for siGemin4#356, 5′-UCU CGG AGA GGA UGC UGU CUC UCU U-3′; for siGemin6#950, 5′-CCC UUA GAA UGG CAA GAU UAC AUU U-3′; for siGemin6#951, 5′-GCA AAG CAU ACA GCC CAG AGG AUC U-3′; and for siGemin6#952, 5′-UCU GUC GCG UGU UCA GGA UCU UAU U-3′.

Transfection of siRNA. Cells were transfected with 40 nM of siRNA (siGemin2 or siGFP) by use of Oligofectamine or Lipofectamine 2000 (Invitrogen, CA). After 4 h of incubation, the cells transfected with the siRNA were added to 250 μl DMEM supplemented with 30% (vol/vol) heat-inactivated FBS. After 12 to 18 h of incubation, the transfected cells were washed and replaced with DMEM supplemented with 10% (vol/vol) heat-inactivated FBS, 100 units/ml penicillin G, and 100 μg/ml streptomycin sulfate. After 24 h of incubation, the siRNA duplex was transfected again to achieve efficient depletion of the target protein.

Virus preparation and infection. Pseudotyped viruses were generated as described previously (29). Briefly, 293T cells were transfected with the pNL43lucΔenv vector together with an ampho-MLV (pJD-1) (29) or vesicular stomatitis virus-G expression vector (pHCMVG) (40) by use of Lipofectamine (Invitrogen). The culture supernatants of the transfected cells (5 ml) were harvested 48 h posttransfection, filtered through 0.45-mm-pore-size filters, and used as virus preparations. The virus preparation was treated with DNase I (Worthington, Lakewood, NJ) (20 μg/ml) in the presence of 10 mM $MgCl_2$ at 37°C for 40 min to avoid plasmid DNA contamination. An aliquot of the virus preparation was incubated at 65°C for 30 min and used as a heat-inactivated control. To monitor the amount of virus in each preparation, HIV-1 p24 antigen levels were determined using an enzyme-linked immunosorbent assay. To monitor viral gene expression from each plasmid vector, luciferase activity in the transfected cells was also measured. At 48 h posttransfection, the 293T cells were lysed with 1 ml of 1× cell culture lysis reagent (Promega, Madison, WI), and 10 μl of each cell lysate was subjected to the luciferase assay. After incubation for 6 h, the viruses were removed and the cells were washed and incubated with fresh culture medium at 37°C in a 5% CO_2 incubator.

Analysis of HIV-1 cDNA synthesis. Total cells were harvested from each well periodically after infection with pseudotyped viruses. After washes with phosphate-buffered saline (PBS), total DNA was extracted by the urea-lysis method (29). Quantitative analyses of the amplified products and the rate of viral cDNA synthesis were performed using real-time quantitative PCR (LightCycler; Roche Diagnostics, Mannheim, Germany) as described previously (20).

Antibodies. The anti-Gemin2 monoclonal antibody (MAb), the anti-Ran MAb, and the anti-SMN MAb were purchased from BD Bioscience. The anti-Gemin3 MAb was purchased from ImmuQuest (ImmuQuest Ltd., Barwick TS175AL, United Kingdom). The anti-Gemin4 and anti-Gemin6 MAbs were purchased from Santa Cruz Biotechnology Inc. (Santa Cruz, CA). Anti-HIV-1 IN MAb was purchased from Microbix Biosystems Inc. (Toronto, Canada). Anti-HIV-1 p24 MAb was purchased from Chemicon International (Temecula, CA).

GST pull-down assay. DNA fragments encoding the N-terminal (amino acid positions 1 to 55), central (amino acid positions 50 to 212), and C-terminal (amino acid positions 213 to 288) HIV-1 IN regions or full-length (amino acid positions 1 to 288) HIV-1 IN were amplified by PCR using pNL43lucΔenv as a template. The amplified products were ligated to BamHI-EcoRI-digested pGEX-2T vector (Amersham Pharmacia Biosciences Inc., Uppsala, Sweden). Recombinant glutathione-*S*-transferase (GST)–IN was prepared as described previously (20). HeLa cell lysate (100 to 200 μg) was incubated with each GST-IN protein (200 nM) immobilized on glutathione-Sepharose beads in binding buffer (1.0% Triton X-100-1 mM phenylmethylsulfonyl fluoride in 1× PBS) for 15 min at 4°C. The beads were then washed five times with wash buffer (0.3% Triton X-100 in 1× PBS) and eluted with elution buffer. An aliquot of the pulled-down fraction was subjected to sodium dodecyl sulfate–12% polyacrylamide gel electrophoresis and Western blotting analysis.

Immunoprecipitation experiments. Total cell extracts were prepared as described previously (34). Briefly, cell pellets were suspended in RSB-100 (10 mM Tris-HCl [pH 7.4], 2.5 mM $MgCl_2$, 100 mM $NaCl_2$) containing 0.1% Nonidet P-40 and protease inhibitors followed by centrifugation at 10,000 × g for 15 min. Extracts were incubated with an anti-FLAG antibody (Sigma) for 1 h and subjected to immunoprecipitation using the Catch and Release system according to the manufacturer's instructions (Upstate, Lake Placid, NY).

RESULTS

Identification of a cellular factor that binds to HIV-1 IN. To identify host proteins that bind to HIV-1 IN, we used the yeast two-hybrid system and the yeast-mating method (BD Biosciences, San Jose, CA). A plasmid carrying the entire HIV-1 IN fused with the GAL4 DNA binding domain-coding region (pGBT-IN) was used as a bait vector. Five positive-testing clones were obtained from ~2×10^7 prey plasmids containing a human HeLa cDNA library expressed as GAL4 activation domain fusion proteins. DNA sequence analysis of three of these positive-testing clones resulted in identification of a single cDNA clone encoding an amino acid fragment corresponding to residues 137 to 238 of SMN-interacting protein 1 (Gemin2; formerly SIP1) (26). We therefore termed residues 137 to 238 of Gemin2 IBDG2 (for "IN binding region of Gemin2"). Various bait vectors carrying the full-length or truncated forms of HIV-1 IN were cotransformed with the GAL4 activation domain vector carrying IBDG2 (pGAD-IBDG2) into yeast strain AH109 or HF7c. HIV-1 IN comprises three distinct functional domains (10, 38). Deletion of the COOH-terminal domain of IN (pGBT-DC-IN) significantly reduced the binding of IN to IBDG2, whereas deletion of the NH_2-terminal domain of IN (pGBT-DN-IN) had little effect on the binding activity (Fig. 1A). Deletion of both the NH_2-terminal and the COOH-terminal domains (pGBT-DN/DC-IN) resulted in low-level but significant binding to IBDG2. These results suggest that the COOH-terminal domain of the IN is the minimum domain responsible

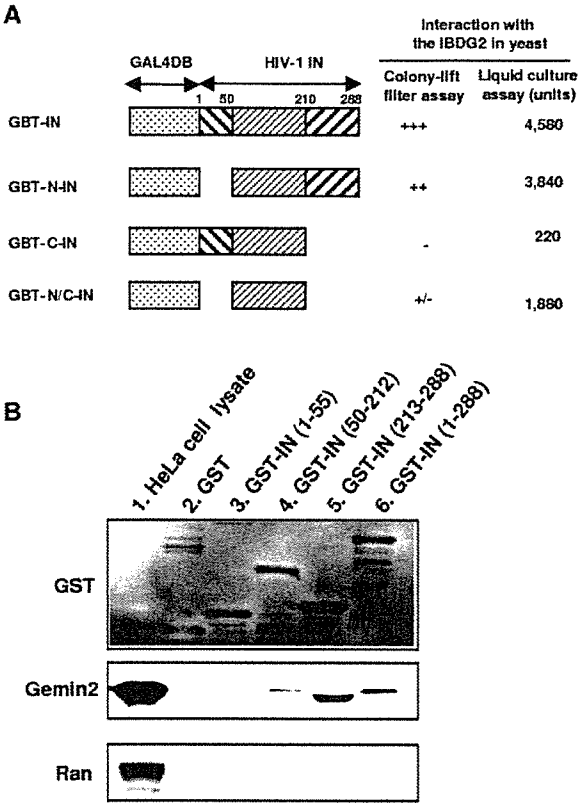

FIG. 1. Interaction of IN with Gemin2. (A) Yeast AH109 or HF7c cells were cotransformed with the pGAD-IBDG2 vector carrying the IBDG2 domain of Gemin2 together with various pGBT9 plasmids carrying full-length (pGBT-IN) or truncated (pGBT-DN-IN, pGBT-DC-IN, and pGBT-DN/DC-IN) forms of HIV-1 IN. Dashed boxes in the diagram indicate the region of HIV-1 IN retained in each pGBT-IN vector. The amino acid positions of HIV-1 IN are numbered according to the NL43 sequence. Interaction of coexpressed proteins was determined with a beta-galactosidase colony-lift filter assay (+++, dark-blue colony; +, medium-blue colony; +/−, light-blue colony; −, white colony) or a liquid-culture assay for estimating beta-galactosidase activity (expressed in units). The value for bait vector only (pGBT-IN) was used as the background value for the liquid-culture assay. (B) Untreated (lane 1) or pull-down (lanes 2 to 6) fractions of HeLa cell lysates on glutathione-Sepharose beads bound to GST-IN protein containing the N-terminal (1-55), central (50-212), C-terminal (213-288), or full-length (1-288) HIV-1 IN were subjected to Western blotting analysis using anti-GST, anti-Gemin2, and noninteracting (control) anti-Ran antibodies.

for the binding to the IBDG2 and that the central domain of IN partly contributed to the binding. We next examined the specific interaction of HIV-1 IN with endogenous Gemin2 in human cells. Recombinant GST fused with the entire IN protein or with the NH_2-terminal, central core, or COOH-terminal domain of HIV-1 IN was used for the pull-down experiment (Fig. 1B). Neither the NH_2-terminal domain of IN (GST-IN1-55) nor the control GST showed any specific binding activity to the endogenous Gemin2; however, the COOH-terminal domain of IN (GST-IN213-288) and full-length IN (GST-IN1-288) each bound to Gemin2. The central core domain of IN (GST-IN55-212) also bound to Gemin2 but with much weaker affinity than the COOH-terminal domain (GST-IN213-288). Thus, we confirmed that HIV-1 IN interacts specifically with full-length Gemin2 endogenously expressed in human cells.

Interaction of Gemin2 with IN of HIV-1 preintegration complex. Gemin2 interacts tightly with the SMN protein to form a macromolecular complex termed the SMN complex (26, 35). To address the interaction of Gemin2 and HIV-1 IN during the viral infection cycle, we first measured the amounts of Gemin2 and other constituents of the SMN complex (SMN and Gemin3) (6, 26) in purified, cell-free virus particles. None of these proteins were detected in the virus particles (Fig. 2A), suggesting that Gemin2 was not incorporated into HIV-1 virus particles. We next used coimmunoprecipitation to address the interaction of Gemin2 and IN during acute infection of HIV-1. Since the antibodies for Gemin2 or HIV-1 IN were available only for immunoblotting but not for immunoprecipitation, we used a lentivirus-vector gene delivery system to transduce FLAG-tagged Gemin2 (34) into HeLa cells (Fig. 2B). The HeLa cells expressing FLAG-tagged Gemin2 (Flag-Gemin2/HeLa) or control HeLa cells transduced with empty vector were infected with HIV-1 pseudotype virus. At 2 or 6 h postinfection, IN efficiently coimmunoprecipitated with FLAG-Gemin2 in the Flag-Gemin2/HeLa cell extract (Fig. 2C), and a significant amount of HIV-1 cDNA synthesized de novo was detected by PCR at each time point. The HIV-1 cDNA in the similarly prepared immunoprecipitate (IP) fraction from the control HeLa cells was below the detectable level following infection (Fig. 2D, upper panel). Quantitative PCR analysis of the HIV-1 cDNA in the IP fraction of the Flag-Gemin2/HeLa cells at 2 h and 6 h postinfection showed that 1,200 and 2,500 copies were present, respectively (Fig. 2D, lower panel), corresponding to 10% to 20% of the total cDNA in the input fraction at each time point. These results suggest that Gemin2 might interact with an incoming HIV-1 preintegration complex through IN after the entry and uncoating of viral genome.

Functional role of Gemin2 during the HIV-1 cycle. We next addressed the functional role of Gemin2 during the HIV-1 infection cycle by using the siRNA technique (36) to specifically deplete Gemin2 from cells. We directed the 21-nucleotide siRNA duplexes (9) against a coding region of the Gemin2 gene (siGemin2). The level of Gemin2 was monitored periodically after siRNA transfection. A reduction in the Gemin2 level was evident 1 day after the siRNA transfection and persisted for at least 4 days in culture (data not shown). At 48 h post-siRNA transfection, the siGemin2 specifically reduced the level of Gemin2 to from 20% to 40% of the level seen with the mock-treated or negative-control siGFP-treated HeLa cells (Fig. 3A). Slight reductions in levels of the SMN complex constituents, SMN and Gemin3 (6), were also noticed following the siGemin2 treatment.

Since the SMN complex regulates the biogenesis of the snRNP complex, we first examined the effects of siGemin2 on gene expression from the HIV-1 provirus and the infectivity of progeny viruses. siGemin2 or a control siGFP duplex (siCont) was cotransfected into 293T cells with an HIV-1 molecular clone, pNL43lucΔenv, and a vector expressing an amphotropic MLV or vesicular stomatitis virus-G envelope for a subsequent single-round infection assay. We measured the levels of p24 (HIV-1 capsid protein) 48 h after transfection. The amount of HIV-1 p24 in the culture supernatants of the siGemin2-transfected 293T cells was comparable to that in control and siCont-

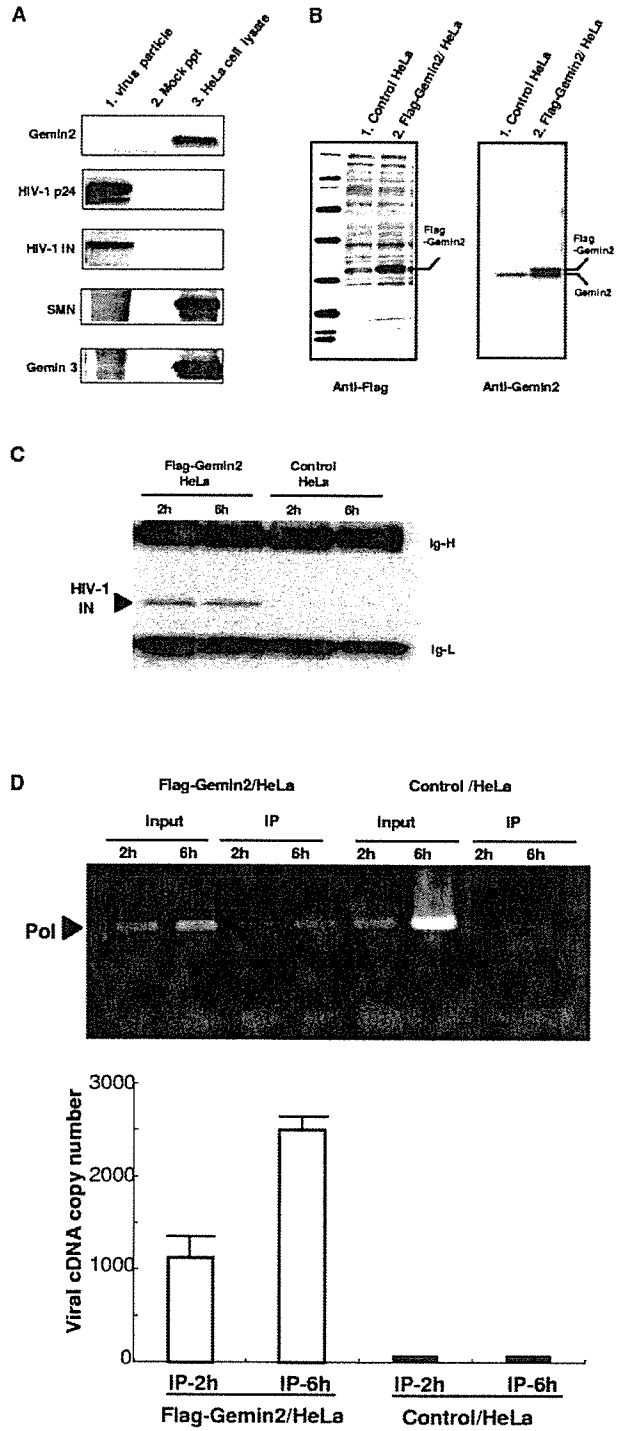

FIG. 2. Gemin2 interacts with the incoming HIV-1 genome complex. (A) Virus particles in the culture supernatant of 293T cells cotransfected with pNL43lucΔenv and pHCMVG were pelleted by ultracentrifugation (1 h at 315,000 × *g*) and subjected to Western blotting analysis using anti-Gemin2, anti-HIV-1 IN, or anti-p24 antibodies. Similarly prepared pellet fractions from mock-transfected cell supernatants (Mock ppt) and a HeLa whole-cell lysate were used as negative and positive controls, respectively. (B) HeLa cells were transduced with an empty vector (Control HeLa) or a FLAG-tagged Gemin2-expressing lentiviral vector (Flag-Gemin2/HeLa) and then subjected to Western blotting using an anti-FLAG antibody (left panel) or anti-Gemin2 antibody (right panel). (C) The transduced HeLa cells were infected with HIV-1 pseudotype virus. At 2 or 6 h postinfection, the cell lysates were immunoprecipitated with an anti-FLAG antibody and then subjected to Western blotting using an HIV-1 IN antibody. IgH, immunoglobulin heavy chain; IgL, immunoglobulin light chain. (D) Nucleic acids extracted from whole-cell lysates (input) or the IP obtained as described for panel C were subjected to PCR analysis of HIV-1 cDNAs. Amplified products (Pol) were separated in a 2% agarose gel and visualized by SYBR green staining (upper). The copy number of viral cDNA (R/gag) in each sample was estimated with real-time quantitative PCR (lower panel). Means ± standard errors (SE) from triplicate assays are shown.

transfected 293T cells (Fig. 3B, left panel). Furthermore, the progeny viruses released from the siGemin2-transfected 293T cell retained their infectivity (Fig. 3B, right panel). Thus, depletion of Gemin2 did not lead to any significant effect on proviral gene expression, virus release, or subsequent viral infectivity.

In contrast, HIV-1 infectivity was significantly reduced when the siGemin2 duplex was introduced into cells before viral infection (Fig. 3C). To exclude nonspecific or off-target effects (22) of the siGemin2 duplex originally tested here, we used four additional chemically modified synthetic siRNA duplexes (Stealth RNAi; Invitrogen) targeting different sequences within Gemin2 (Gemin2#372, Gemin2#373, Gemin2#374, and Gemin2#375) and an siGemin2 duplex carrying several nucleotide substitutions as a mismatch siGemin2 control (mm375). We observed significant reductions of HIV-1 infectivity that correlated well with the amount of specific reduction of Gemin2 with each type of siRNA treatment (Fig. 3C). In addition, we constructed an siRNA-resistant Gemin2 expression vector carrying silent point mutations in the target sequences of siGemin2#372. The siRNA-resistant Gemin2 continued to be expressed in the presence of siGemin2#372, but expression of the endogenous Gemin2 was greatly reduced (Fig. 3D lower). Under this condition, the siRNA-resistant Gemin2 rescued HIV-1 infectivity in siGemin2-treated cells (Fig. 3D upper). These results strongly suggest the functional role of Gemin2 through interaction with incoming HIV-1 genome complexes during the early steps of HIV-1 infection.

Functional role of Gemin2 in HIV-1 infection of primary nondividing cells. Next, we addressed the functional role of Gemin2 in HIV-1 infection of human primary MDMs, a model of major natural targets for HIV-1 infection in vivo. MDMs were isolated from three different healthy donors. Transfection of siGemin2 into MDMs markedly reduced HIV-1 infectivity to from 0.3% to 10% of the levels in the control MDMs (Fig. 4B, left panel). This remarkable effect of siGemin2 observed in MDMs could be partly explained by the fact that primary MDMs constitutively express a lower level of Gemin2 than the 293T and HeLa cell lines, which have been adapted in vitro (Fig. 4A). We confirmed that reduction of Gemin2 also suppressed spreading of replication-competent HIV-1 in MDMs to less than 10% of control level for at least 7 days (data not shown). As with the results obtained using 293T and HeLa cell lines, the siGemin2 duplex did not significantly affect HIV-1 expression when introduced into MDMs 24 h after infection (Fig. 4B, right panel).

Finally, we addressed the effect of depletion of Gemin2 on HIV-1 cDNA synthesis and subsequent integration using real-

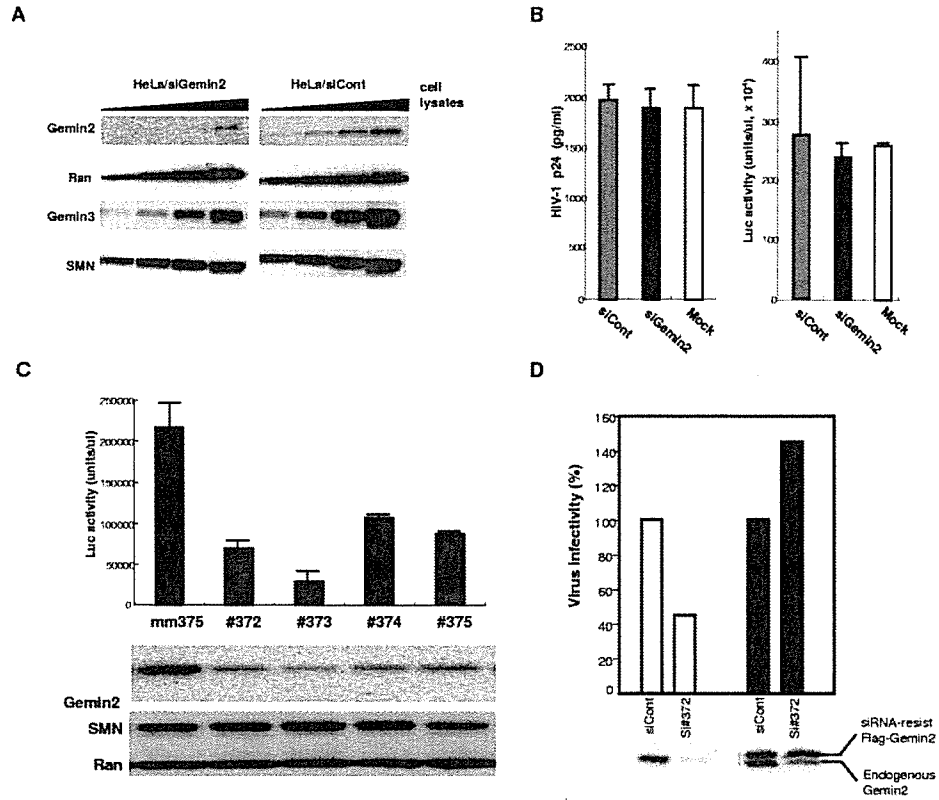

FIG. 3. Involvement of cellular Gemin2 in HIV-1 replication. (A) Total HeLa cell lysates prepared 48 h after transfection of siGemin2 (HeLa/siGemin2) or control siGFP (HeLa/siCont) were serially diluted twofold followed by Western blot analysis with antibodies against Gemin2, Ran, Gemin3, and SMN. (B) 293T cells were transfected with siGemin2 (black bar), siGFP (siCont; gray bar), or no siRNA (Mock; white bar), together with pNL-lucΔenv vector and pJD-1. The level of virus release from these 293T cells was determined by measuring HIV-1 p24 concentrations in the culture supernatant (left panel) 48 h posttransfection. These virus-containing supernatants were then incubated with HeLa cells. The cells were harvested 48 h postinfection and subjected to a luciferase assay (right panel). (C) HeLa cells were transfected with Stealth-siGemin2 (#372, #373, #374, or #375) or the control mismatch siGemin2 (mm375) 48 h before infection with HIV-1 pseudotype virus. The cells were harvested 48 h postinfection and subjected to a luciferase assay (upper panel) and Western blotting for Gemin2, SMN, and Ran (lower panel). (D) 293T cells were transfected with siRNA-resistant Flag-Gemin2 expression vector (black bars) or control empty vector (white bars) together with siGemin2#372 (si#372) or control siRNA (siCont) and then infected with HIV-1 pseudotype virus. The cells were harvested 24 h postinfection and subjected to a luciferase assay (upper) and Western blotting for endogenous Gemin2 and Flag-Gemin2 (lower). Virus infectivity is presented relative to the Luc activity in siCont-transfected cells, which was set to 100%.

time quantitative PCR analysis (20) in MDMs. Over time, the level of late reverse-transcription products (R/gag) was reduced in siGemin2-treated MDM (Fig. 4C) to ~5% of the level in the control siRNA-treated MDM at 48 h after HIV-1 infection (Fig. 4D). Of note, the amount of the early products of reverse transcription (R/U5) in the siGemin2-treated MDM was 30% to 40% of the level in the control siGFP-treated MDM (Fig. 4D). The region amplified for detection of the early reverse-transcription products (R/U5) is duplicated in the complete or nearly complete form of viral cDNA (late reverse transcription; R/gag) during the reverse-transcription step. Therefore, the marked reduction in the late reverse-transcription products by siGemin2 would be in part a consequence of the reduction in the duplication of the R/U5 region. The reduced amounts of the two-long terminal repeat (2-LTR) or integrated forms of cDNA observed in the siGemin2-treated MDMs could also be attributed to the inhibition of viral cDNA synthesis (2-LTR and integration; Fig. 4D). Thus, the dramatic reduction in the levels of late reverse-transcription products in the siGemin2-treated MDMs indicates that the abrogation of the reverse transcription of viral RNA might occur before or during the second template switch needed to complete the double-stranded viral cDNA copy, suggesting a role for Gemin2 during reverse transcription of the HIV-1 genome in vivo. We also confirmed that siGemin2 produced a similar effect on late RT products in HeLa cells. However, the inhibitory effect of siGemin2 on late RT products in HeLa cells was weaker than that in MDMs (data not shown). Therefore, possible roles of Gemin2 at other steps, including nuclear transport and integration of viral cDNA, cannot be ruled out.

Involvement of other constituents of the SMN complex. Under our experimental conditions, reduction of Gemin2 by siGemin2 was accompanied by slight decreases in SMN and Gemin3 levels (Fig. 3A and 4A). We addressed the critical point of whether Gemin2 acts on HIV-1 through the SMN complex or through another, unknown, complex by use of siRNAs targeting the other Gemin2-related proteins constituting the SMN complex. For each constituent of the complex—SMN (26), Gemin3 (6), Gemin4 (7), and Gemin6 (34)—we synthesized two or three chemically modified siRNA duplexes

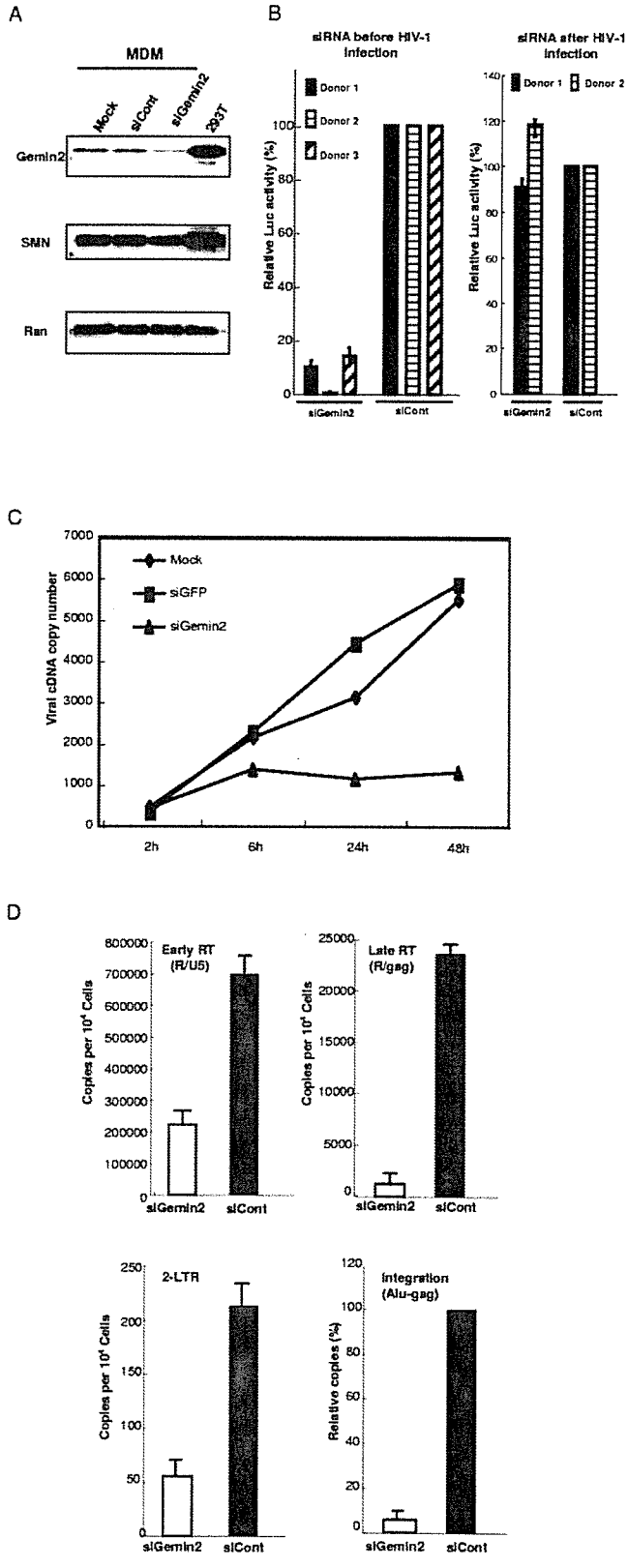

FIG. 4. Effect of siGemin2 on HIV-1 infection and cDNA synthesis in primary MDMs. (A) MDMs were transfected with siGemin2 or control siGFP (siCont) and subjected to Western blot analysis for Gemin2, SMN, and Ran. Mock, mock infected. (B) MDMs were transfected with each siRNA 24 h before (left panel) or after (right panel) infection with HIV-1 pseudotype virus. Cells were harvested and subjected to a luciferase assay 48 h (left panel) or 72 h (right panel) after infection. Relative Luc activity was calculated as a percentage of the control value in siCont-transfected cells. Each bar represents the value determined using MDMs prepared from different donors. Means ± SE from duplicate assays are shown. (C) MDMs were transfected with each siRNA 24 h before HIV-1 infection. Total DNA was extracted from siGemin2- or control siGFP-transfected MDMs at 2, 6, 24, and 48 h postinfection. Each sample was subjected to a quantitative analysis of viral cDNAs using real-time quantitative PCR with the primer pair M667-M661 (R/gag region) to measure the amount of complete or nearly complete viral cDNA (late RT). (D) Total DNA was extracted from MDMs transfected with siGemin2 or siGFP (siCont), infected with HIV-1 pseudotype virus for 48 h, and subjected to a quantitative analysis of viral cDNAs by use of real-time quantitative PCR with primer pair M667-AA55 (R/U5 region) for viral cDNA (Early-RT) or primer pair M667-M661 (R/gag region) for complete or nearly complete viral cDNA (Late-RT). We also monitored the formation of 2-LTR circular DNA by use of a primer pair that amplifies a sequence unique to the 2-LTR DNA junction and monitored the level of the integrated form of each viral cDNA by the Alu-PCR method using HIV-1-specific (M661) and Alu (Integration) primers. Results represent means ± SE.

targeting different sites within the coding sequence. Then we evaluated the effects of each siRNA on HIV-1 infection in HeLa cells (Fig. 5A). In parallel, the specific reduction in protein caused by each siRNA was also determined by examining protein expression profiles of the SMN constituents (Fig. 5B). Reduction of Gemin2 or SMN significantly blocked HIV-1 infection without showing apparent cell toxicity. However, siRNA duplexes against the SMN also significantly reduced Gemin2 levels (siSMN#271 and siSMN#272; Fig. 5B). In repeated experiments, the inhibitory effects of siSMNs on HIV-1 always correlated with the level of indirect reduction of Gemin2. Meanwhile, the reduction of Gemin3, Gemin4, and Gemin6 levels through their respective siRNA duplexes did not significantly affect HIV-1 infectivity, although siGemin3#432 and siGemin6#950 did inhibit HIV-1 infection by causing high cell toxicity. These results suggest that among the SMN constituents, Gemin2 is a critical constituent necessary to support HIV-1 infection. Thus, the effect of Gemin2 on HIV-1 infectivity might be independent of the other constituents of the SMN complex.

DISCUSSION

In this study, we have provided evidence that a novel host protein binds to HIV IN and modulates HIV-1 cDNA synthesis in vivo. We identified residues 137 to 238 of Gemin2 as binding to IN. In both the yeast two-hybrid system and a GST pull-down assay, the COOH-terminal domain of the IN was shown to be the minimum domain responsible for binding to Gemin2 (Fig. 1), although the central domain of the IN partly contributed to the binding. Gemin2 is a constituent of the SMN complex, along with other Gemin family proteins, including the putative DEAD box helicase dp103/Gemin3 (6), Gemin4 (7), Gemin5 (18), Gemin6 (34), and Gemin7 (2). Under our experimental conditions, treatment of cells with siGemin2 reduced the amount of Gemin2 protein and also resulted in slight decreases of SMN and Gemin3 levels (Fig. 3A and 4A).

Although the exact role of Gemin2 in the snRNP complex

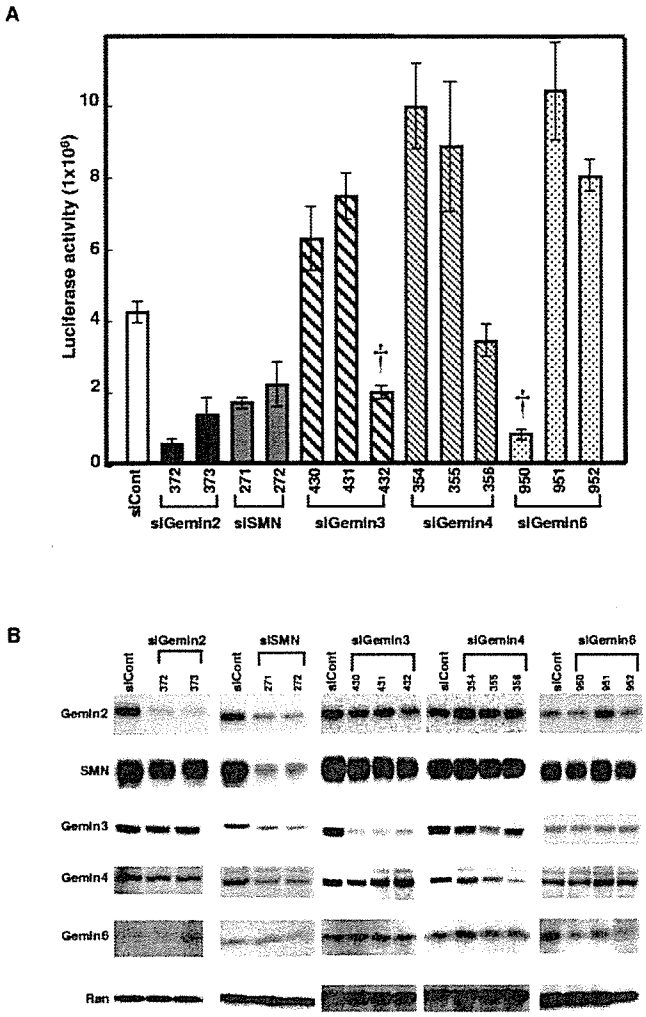

FIG. 5. Involvement of other constituents of the SMN complex. (A) HeLa cells were transfected with the Stealth siRNAs targeting Gemin2, Gemin3, Gemin4, Gemin6, or SMN 48 h before infection with HIV-1 pseudotype virus. The mismatch siGemin2 (mm375) was used as a negative control siRNA (siCont). The cells were harvested 48 h postinfection and subjected to a luciferase assay. Each bar represents the means ± SE. †, less than 20% of cells were viable 48 h after siRNA transfection. (B) Aliquots of the same cells harvested for the luciferase assay as described for panel A were subjected to Western blot analysis for Gemin2, SMN, Gemin3, Gemin4, Gemin6, and Ran.

remains to be determined, some reports suggest that it has a critical role in the assembly of the snRNP complex in the cytoplasm (3, 21, 30). More recently, the roles of the individual SMN constituents were addressed by using RNA interference (14). Feng et al. showed that a reduction of SMN leads to a decrease in snRNP assembly, the disappearance of bodies called Gems where SMN and Gemin2 are concentrated in the nucleus, and a drastic reduction in the amounts of several Gemins. Moreover, reduction of Gemin2 or Gemin6 levels strongly decreases the activity of the SMN complex. Therefore, we cannot exclude the possibility that a reduction of Gemin2 might also reduce SMN function under our experimental conditions. However, our data obtained using siRNAs targeting SMN, Gemin3, Gemin4, or Gemin6 suggest that Gemin2 is a critical constituent of the SMN complex for support of HIV-1 infection (Fig. 5). It seems likely that Gemin2 acts on the HIV-1 preintegration complex, either alone or with as-yet-unknown proteins other than the SMN constituents, although this point remains to be confirmed. In addition to the full-length Gemin2 (termed Gemin2-alpha), three splicing variants of Gemin2 (Gemin2-beta, -gamma, and -delta) have been identified (1). Gemin2-alpha has found to be ubiquitously expressed at high levels in the various normal tissues. In contrast, Gemin2-beta and -gamma are expressed at very low levels in these normal tissues (1). The Gemin2 residues that we identified as the region of Gemin2 that binds IN in the yeast two-hybrid system (residues 137 to 238, IBDG2) were shared by all splicing variants of Gemin2 except Gemin2-beta, in which residues 174 to 188 are deleted. It will be interesting to identify the contribution of other splicing variants of Gemin2 to HIV-1 infection.

The SMN complex has recently been reported to be generally used by infectious agents for RNP assembly (17). Golembe et al. demonstrated that herpesvirus saimiri uses the SMN complex to assemble Sm cores on its small RNAs (HSURs), just as occurs with host snRNPs. HSURs are the most abundant viral transcripts in latently infected, transformed T cells but are not essential for viral replication. Thus, the biological meaning of their complex formation remains to be determined. However, the authors suggest that infectious agents that engage the SMN complex may burden SMN-dependent pathways, possibly leading to a deleterious reduction in the availability of SMN complexes for essential host functions.

In the case of HIV-1 infection, we showed here that HIV-1 might require Gemin2 for efficient viral cDNA synthesis. Our results suggest that Gemin2, either alone or in concert with unidentified cellular proteins, supports HIV-1 infection, probably by supporting the reassembly of the reverse transcription complex to initiate and complete reverse transcription. Several cases of mutations in HIV-1 IN affecting reverse transcription have been described previously (11, 29, 37, 39, 42). It is, therefore, reasonable that a protein interacting with IN might play a role in reverse transcription and could also be involved in the subsequent nuclear transport and integration of viral cDNA. Since both reverse transcription and integration are essential steps for retrovirus infection, our findings will shed light on the functional role of IN during the reverse transcription of the retroviral genome and will also serve as the basis for a novel therapeutic approach to treat HIV-1 disease.

ACKNOWLEDGMENTS

We thank G. Dreyfuss for providing pTRE-FLAG-GEMIN2; I. S. Y. Chen for pNL43lucΔenv, pJD-1, and pHCMVG; and H. Miyoshi for pCSII-CMV-MCS. We also thank Y. Kawaguchi for technical advice on the yeast two-hybrid system and M. Kubo, S. Kaiga, N. Takahashi, M. Mogi, and S. Nishino for their technical assistance.

This work was supported by a Grant-in-Aid for Scientific Research on Priority Areas from the Ministry of Education, Culture, Sports, Science and Technology (MEXT) of Japan and a Health Sciences Research Grant from the Ministry of Health, Labor and Welfare of Japan (Research on HIV/AIDS13110201).

REFERENCES

1. **Aerbajinai, W., T. Ishihara, K. Arahata, and T. Tsukahara.** 2002. Increased expression level of the splicing variant of SIP1 in motor neuron diseases. Int. J. Biochem. Cell Biol. 34:699–707.

2. **Baccon, J., L. Pellizzoni, J. Rappsilber, M. Mann, and G. Dreyfuss.** 2002. Identification and characterization of Gemin7, a novel component of the survival of motor neuron complex. J. Biol. Chem. **277:**31957–31962.
3. **Buhler, D., V. Raker, R. Luhrmann, and U. Fischer.** 1999. Essential role for the tudor domain of SMN in spliceosomal U snRNP assembly: implications for spinal muscular atrophy. Hum. Mol. Genet. **8:**2351–2357.
4. **Bukrinsky, M. I., and O. K. Haffar.** 1997. HIV-1 nuclear import: in search of a leader. Front Biosci. **2:**d578–d587.
5. **Bukrinsky, M. I., N. Sharova, T. L. McDonald, T. Pushkarskaya, W. G. Tarpley, and M. Stevenson.** 1993. Association of integrase, matrix, and reverse transcriptase antigens of human immunodeficiency virus type 1 with viral nucleic acids following acute infection. Proc. Natl. Acad. Sci. USA **90:**6125–6129.
6. **Charroux, B., L. Pellizzoni, R. A. Perkinson, A. Shevchenko, M. Mann, and G. Dreyfuss.** 1999. Gemin3: a novel DEAD box protein that interacts with SMN, the spinal muscular atrophy gene product, and is a component of gems. J. Cell Biol. **147:**1181–1194.
7. **Charroux, B., L. Pellizzoni, R. A. Perkinson, J. Yong, A. Shevchenko, M. Mann, and G. Dreyfuss.** 2000. Gemin4. A novel component of the SMN complex that is found in both gems and nucleoli. J. Cell Biol. **148:**1177–1186.
8. **Cullen, B. R.** 2001. Journey to the center of the cell. Cell **105:**697–700.
9. **Elbashir, S. M., J. Harborth, W. Lendeckel, A. Yalcin, K. Weber, and T. Tuschl.** 2001. Duplexes of 21-nucleotide RNAs mediate RNA interference in cultured mammalian cells. Nature **411:**494–498.
10. **Engelman, A., F. D. Bushman, and R. Craigie.** 1993. Identification of discrete functional domains of HIV-1 integrase and their organization within an active multimeric complex. EMBO J. **12:**3269–3275.
11. **Engelman, A., G. Englund, J. M. Orenstein, M. A. Martin, and R. Craigie.** 1995. Multiple effects of mutations in human immunodeficiency virus type 1 integrase on viral replication. J. Virol. **69:**2729–2736.
12. **Fassati, A., and S. P. Goff.** 2001. Characterization of intracellular reverse transcription complexes of human immunodeficiency virus type 1. J. Virol. **75:**3626–3635.
13. **Fassati, A., and S. P. Goff.** 1999. Characterization of intracellular reverse transcription complexes of Moloney murine leukemia virus. J. Virol. **73:**8919–8925.
14. **Feng, W., A. K. Gubitz, L. Wan, D. J. Battle, J. Dostie, T. J. Golembe, and G. Dreyfuss.** 2005. Gemins modulate the expression and activity of the SMN complex. Hum. Mol. Genet. **14:**1605–1611.
15. **Fischer, U., Q. Liu, and G. Dreyfuss.** 1997. The SMN-SIP1 complex has an essential role in spliceosomal snRNP biogenesis. Cell **90:**1023–1029.
16. **Goff, S. P.** 2001. Intracellular trafficking of retroviral genomes during the early phase of infection: viral exploitation of cellular pathways. J. Gene Med. **3:**517–528.
17. **Golembe, T. J., J. Yong, D. J. Battle, W. Feng, L. Wan, and G. Dreyfuss.** 2005. Lymphotropic *Herpesvirus saimiri* uses the SMN complex to assemble Sm cores on its small RNAs. Mol. Cell. Biol. **25:**602–611.
18. **Gubitz, A. K., Z. Mourelatos, L. Abel, J. Rappsilber, M. Mann, and G. Dreyfuss.** 2002. Gemin5, a novel WD repeat protein component of the SMN complex that binds Sm proteins. J. Biol. Chem. **277:**5631–5636.
19. **Hehl, E. A., P. Joshi, G. V. Kalpana, and V. R. Prasad.** 2004. Interaction between human immunodeficiency virus type 1 reverse transcriptase and integrase proteins. J. Virol. **78:**5056–5067.
20. **Ikeda, T., H. Nishitsuji, X. Zhou, N. Nara, T. Ohashi, M. Kannagi, and T. Masuda.** 2004. Evaluation of the functional involvement of human immunodeficiency virus type 1 integrase in nuclear import of viral cDNA during acute infection. J. Virol. **78:**11563–11573.
21. **Jablonka, S., M. Bandilla, S. Wiese, D. Buhler, B. Wirth, M. Sendtner, and U. Fischer.** 2001. Co-regulation of survival of motor neuron (SMN) protein and its interactor SIP1 during development and in spinal muscular atrophy. Hum. Mol. Genet. **10:**497–505.
22. **Jackson, A. L., S. R. Bartz, J. Schelter, S. V. Kobayashi, J. Burchard, M. Mao, B. Li, G. Cavet, and P. S. Linsley.** 2003. Expression profiling reveals off-target gene regulation by RNAi. Nat. Biotechnol. **21:**635–637.
23. **Kalpana, G. V., S. Marmon, W. Wang, G. R. Crabtree, and S. P. Goff.** 1994. Binding and stimulation of HIV-1 integrase by a human homolog of yeast transcription factor SNF5. Science **266:**2002–2006.
24. **Katz, R. A., and A. M. Skalka.** 1994. The retroviral enzymes. Annu. Rev. Biochem. **63:**133–173.
25. **Leavitt, A. D., G. Robles, N. Alesandro, and H. E. Varmus.** 1996. Human immunodeficiency virus type 1 integrase mutants retain in vitro integrase activity yet fail to integrate viral DNA efficiently during infection. J. Virol. **70:**721–728.
26. **Liu, Q., U. Fischer, F. Wang, and G. Dreyfuss.** 1997. The spinal muscular atrophy disease gene product, SMN, and its associated protein SIP1 are in a complex with spliceosomal snRNP proteins. Cell **90:**1013–1021.
27. **Maertens, G., P. Cherepanov, Z. Debyser, Y. Engelborghs, and A. Engelman.** 2004. Identification and characterization of a functional nuclear localization signal in the HIV-1 integrase interactor LEDGF/p75. J. Biol. Chem. **279:**33421–33429.
28. **Maertens, G., P. Cherepanov, W. Pluymers, K. Busschots, E. De Clercq, Z. Debyser, and Y. Engelborghs.** 2003. LEDGF/p75 is essential for nuclear and chromosomal targeting of HIV-1 integrase in human cells. J. Biol. Chem. **278:**33528–33539.
29. **Masuda, T., V. Planelles, P. Krogstad, and I. S. Chen.** 1995. Genetic analysis of human immunodeficiency virus type 1 integrase and the U3 *att* site: unusual phenotype of mutants in the zinc finger-like domain. J. Virol. **69:**6687–6696.
30. **Meister, G., D. Buhler, R. Pillai, F. Lottspeich, and U. Fischer.** 2001. A multiprotein complex mediates the ATP-dependent assembly of spliceosomal U snRNPs. Nat. Cell Biol. **3:**945–949.
31. **Miyoshi, H., U. Blomer, M. Takahashi, F. H. Gage, and I. M. Verma.** 1998. Development of a self-inactivating lentivirus vector. J. Virol. **72:**8150–8157.
32. **Nakamura, T., T. Masuda, T. Goto, K. Sano, M. Nakai, and S. Harada.** 1997. Lack of infectivity of HIV-1 integrase zinc finger-like domain mutant with morphologically normal maturation. Biochem. Biophys. Res. Commun. **239:**715–722.
33. **Nymark-McMahon, M. H., N. S. Beliakova-Bethell, J. L. Darlix, S. F. Le Grice, and S. B. Sandmeyer.** 2002. Ty3 integrase is required for initiation of reverse transcription. J. Virol. **76:**2804–2816.
34. **Pellizzoni, L., J. Baccon, J. Rappsilber, M. Mann, and G. Dreyfuss.** 2002. Purification of native survival of motor neurons complexes and identification of Gemin6 as a novel component. J. Biol. Chem. **277:**7540–7545.
35. **Pellizzoni, L., J. Yong, and G. Dreyfuss.** 2002. Essential role for the SMN complex in the specificity of snRNP assembly. Science **298:**1775–1779.
36. **Sharp, P. A.** 2001. RNA interference—2001. Genes Dev. **15:**485–490.
37. **Tsurutani, N., M. Kubo, Y. Maeda, T. Ohashi, N. Yamamoto, M. Kannagi, and T. Masuda.** 2000. Identification of critical amino acid residues in human immunodeficiency virus type 1 IN required for efficient proviral DNA formation at steps prior to integration in dividing and nondividing cells. J. Virol. **74:**4795–4806.
38. **van Gent, D. C., C. Vink, A. A. Groeneger, and R. H. Plasterk.** 1993. Complementation between HIV integrase proteins mutated in different domains. EMBO J. **12:**3261–3267.
39. **Wu, X., H. Liu, H. Xiao, J. A. Conway, E. Hehl, G. V. Kalpana, V. Prasad, and J. C. Kappes.** 1999. Human immunodeficiency virus type 1 integrase protein promotes reverse transcription through specific interactions with the nucleoprotein reverse transcription complex. J. Virol. **73:**2126–2135.
40. **Yee, J. K., T. Friedmann, and J. C. Burns.** 1994. Generation of high-titer pseudotyped retroviral vectors with very broad host range. Methods Cell Biol. **43**(Pt. A):99–112.
41. **Yung, E., M. Sorin, A. Pal, E. Craig, A. Morozov, O. Delattre, J. Kappes, D. Ott, and G. V. Kalpana.** 2001. Inhibition of HIV-1 virion production by a transdominant mutant of integrase interactor 1. Nat. Med. **7:**920–926.
42. **Zhu, K., C. Dobard, and S. A. Chow.** 2004. Requirement for integrase during reverse transcription of human immunodeficiency virus type 1 and the effect of cysteine mutations of integrase on its interactions with reverse transcriptase. J. Virol. **78:**5045–5055.